Supporting Information

Structural bases for mechano-responsive properties in molecular gels of (*R*)-12-hydroxy-*N*-(ω-hydroxyalkyl)octadecanamides. Rates of formation and responses to destructive strain.

V. Ajay Mallia[a] and Richard G. Weiss[a,b*]

[a] Department of Chemistry and [b] Institute for Soft Matter Synthesis and Metrology, Georgetown University, Washington, DC 20057-1227, USA.

Experimental

^{1}H NMR spectra were recorded on a Varian 300 MHz spectrometer and chemical shifts were referenced to an internal standard, tetramethylsilane (TMS). Elemental analyses were performed on a Perkin-Elmer 2400 CHN elemental analyzer using acetanilide as a calibration standard. Melting points and polarized optical micrographs (POMs) were recorded on a Leitz 585 SM-LUX-POL microscope equipped with crossed polars, a Leitz 350 heating stage, a Photometrics CCD camera interfaced to a computer, and an Omega HH503 microprocessor thermometer connected to a J-K-T thermocouple. The samples for POM analyses were flame-sealed in 0.4 or 0.5 mm path-length, flattened Pyrex capillary tubes (VitroCom, Inc.), heated to their liquid phase in a boiling water bath, and cooled according to protocols described below. Powder X-ray diffraction (XRD) patterns of samples were obtained on a Rigaku R-AXIS image plate system with Cu Kα X-rays (λ = 1.54 Å) generated by a Rigaku generator operating at 46 kV and 40 mA with the collimator at 0.5 mm.[1] Data processing and analyses were performed using Materials Data JADE (version 5.0.35) XRD pattern processing software. Samples were sealed in 0.5 mm glass capillaries (W. Müller, Schönwalde, Germany) and diffraction data were collected for 2 h (neat powders) or 10 h (gels). Differential scanning calorimetry (DSC) were performed on a TA 2910 differential scanning calorimeter interfaced to a TA Thermal Analyst 3100 controller under a slow stream of nitrogen flowing through the cell.

Small-angle neutron scattering (SANS) experiments, using neutrons of wavelength $\lambda = 6$ Å, were conducted at the Center for Neutron Research at the National Institute of Standards and Technology (NIST, Gaithersburg, MD, USA) using the NG7 30 m instrument[2] over a set of 3 detector distances (13, 6, and 1 m), providing an overlap between the 3 configurations and, at the end, a range of scattering vectors Q from 0.004 to 0.45 Å^{-1}. Radial averaging of the isotropic 2D arrays was performed using the NIST software package.[3] Rheological measurements were obtained at 25 °C on an Anton Paar Physica MCR 301 strain-controlled rheometer using a Peltier temperature-controller and parallel plates (25 mm diameter). The gap between the plates was 0.5 mm and the data were collected using Rheoplus/32 Service V3.10 software. Before recording data, each sample was placed between the plates of the rheometer and heated to 110 °C to ensure that a solution/sol was present. It was cooled to 10 °C (~20 °C/min) and the temperature was increased to 25 °C and incubated there for 15 min to reform the gel and remove any shear-induced alignment of the fibers.

Materials. (*R*)-12-Hydroxystearic acid (**HSA**, Arizona Chemicals) was purified as reported (mp 80.2-80.3 °C (lit[4] 80.5-81.0 °C)).[5] *(R)*-12-Hydroxy-*N*-propyloctadecanamide (**HS-3**) was prepared according to the previously reported procedure (mp 107.1-107.5 °C (lit[5] mp 107.3-107.4 °C)).[5] Silicone oil (1,1,5,5-tetraphenyl-1,3,3,5-tetramethyltrisiloxane, >95 %; Gelest, Inc.) and isostearyl alcohol (>99 %; FO 180, Nissan Chemical) were used as received. Solvents for syntheses and other liquids for gelation studies were reagent grade or better (Aldrich). Anhydrous THF (Acros Chemicals, dried over Na and distilled prior to use), triethylamine (99.5%, Aldrich) ethanolamine (99 %, Aldrich), 3-aminopropan-1-ol (99 %, Aldrich), 4-aminobutan-1-ol (97 %, Aldrich), 5-aminopropan-1-ol (95 %, Aldrich) and stearic acid (99 %, Aldrich) were used as received.

*Preparation of N-(3-hydroxypropyl)octadecanamide (**S-3-OH**).* Thionyl chloride (0.6 g, 6 mmol) was slowly added to stearic acid (1.0 g, 3.5 mmol) and the mixture was heated at 55 ^{o}C for 2 h under a dry atmosphere. Excess thionyl chloride was removed by distillation (*T* = 74-75 ^{o}C, under dry conditions) and the remaining liquid (stearoyl chloride) was slowly added to 3-aminopropanol (400 mg, 5.3 mmol). The reaction mixture was stirred at room temperature for 10 h and was then poured into 0.2 M aqueous sodium hydroxide solution (25 mL). The precipitate that formed was collected by vacuum filtration and washed with water (5mL x 3) and recrystallized from ethyl acetate to yield 1.0 g (84 %) of white solid, mp 98.1-98.4 ^{o}C (lit[6] 98-99 ^{o}C). ^{1}H-NMR ($CDCl_3$, 300 (MHz): δ 0.88 (m 3H, CH_3) 1.2-1.6 (m, 28H, -CH_2), 2.17 (t, 2H, -$\underline{CH_2}$-CO-), 3.42 (m, 2H, -$\underline{CH}$-NH), 3.63 (m, 2H, -$\underline{CH_2}$-OH) 5.74 (br, 1H, -NH-).

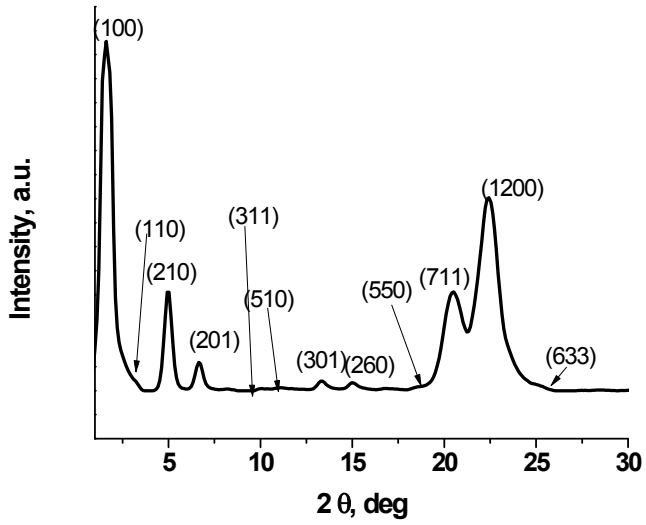

Figure S1. XRD diffractogram of neat **HS-2-OH** at 22 ^{o}C. The numbers in the plot indicate peak indexing.

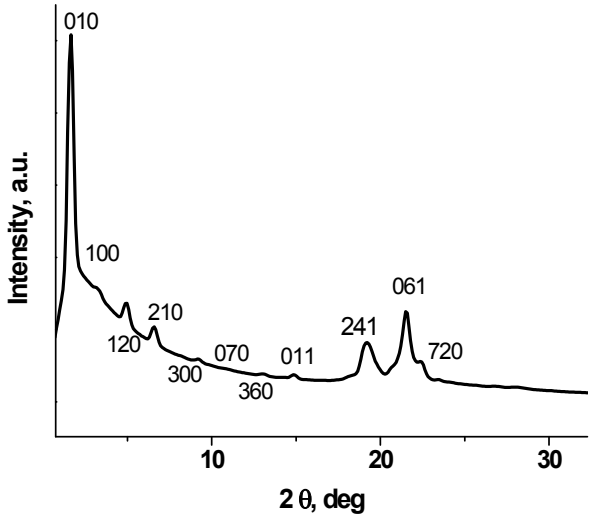

Figure S2. XRD diffractogram of neat **HS-3-OH** at 22 °C. The numbers in the plot indicate peak indexing.

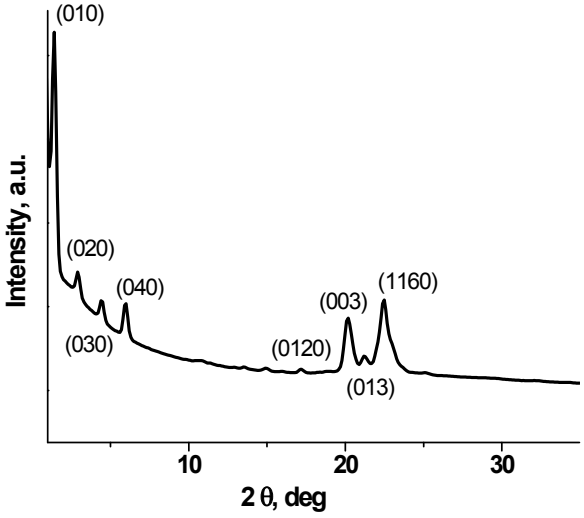

Figure S3. XRD diffractogram of neat **HS-4-OH** at 22 °C. The numbers in the plot indicate peak indexing.

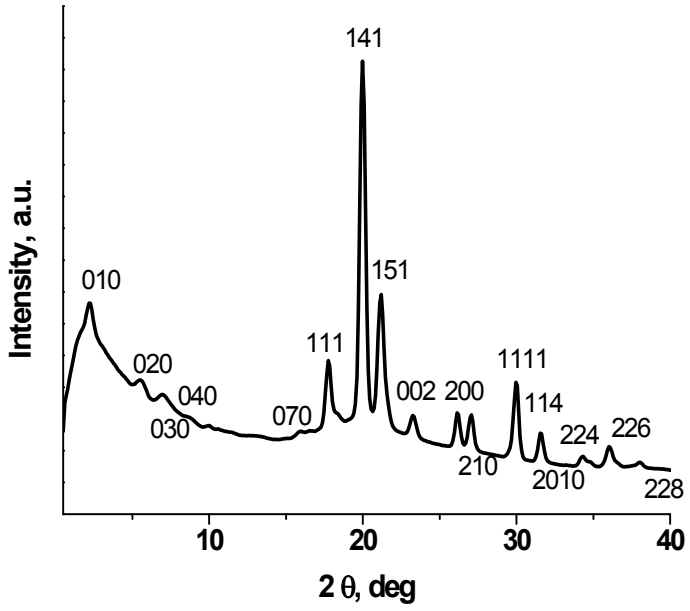

Figure S4. XRD diffractogram of neat **HS-5-OH** at 22 °C. The numbers in the plot indicate peak indexing.

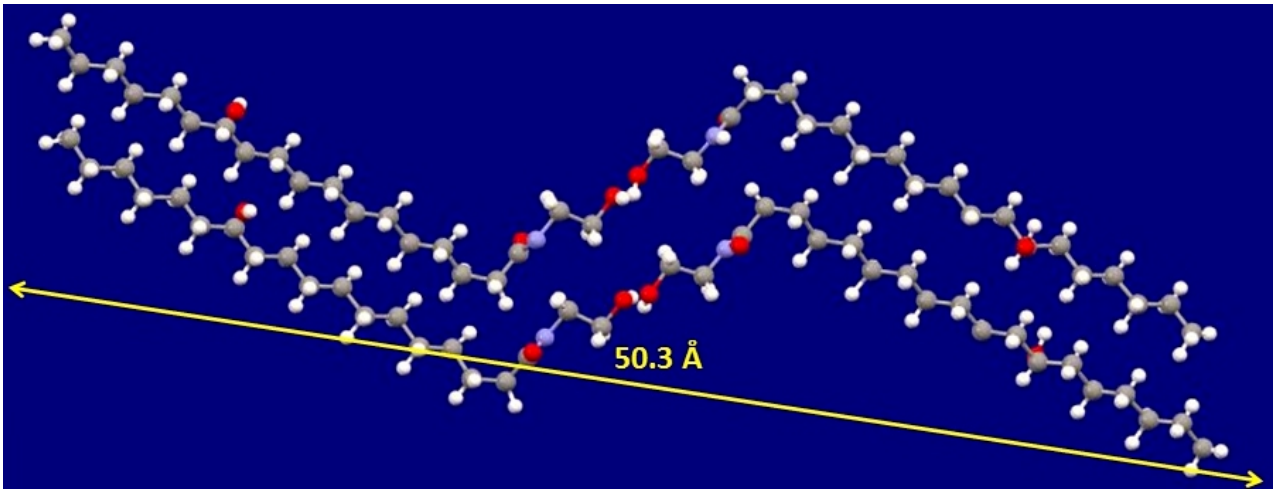

Figure S5. Packing arrangement of **HS-2-OH**,[7] analogous the single crystal packing arrangement reported for N-(2-hydroxyethyl)octadecanamide,[8] and discarded based upon powder XRD data.

Table S1. Bragg spacings (*d*, Å) from pertinent diffraction peaks and refined cell parameters for orthorhombic crystalline packing of **HS-n-OH** in their neat powders (recrystallized from ethyl acetate) and 5 wt % gels from XRD data collected at 22 °C. Calculated extended molecular lengths (*L*, Å)[9] are included as well.

	Cell parameters, Å	*d*, Å	*L*, Å
HS-2-OH (neat)	55 x 26 x 12	54.6, 18.2, 13.6, 6.7, 6.0, 4.4	27.2
5 wt % **HS-2-OH** in toluene gel	-	54.1, 13.1, 6.0, 4,4	
5 wt % **HS-2-OH** in isostearyl alcohol gel	-	54.6, 18.2, 13.6, 6.7, 6.0, 4.4	
HS-3-OH (neat)	28 x 46 x 5	53.8, 26.9, 17.9, 13.4, 9.6, 4.6, 4.1	28.7
5 wt % **HS-3-OH** in toluene gel	-	56.5, 11.7, 4.5, 4.2	
5 wt % **HS-3-OH** in isostearyl alcohol gel	-	55.1, 12.6, 5.2, 4.3, 3.8	
HS-4-OH (neat)	23 x 63 x 13	63.1, 31.6, 15.8, 5.2, 4.3, 4.2, 4.1	30.2
5 wt % **HS-4-OH** in isostearyl alcohol gel	-	67.9, 4.3, 3.9	
HS-5-OH (neat)	40 x 5 x 8	40.1, 16.3, 12.8, 4.9, 4.4	
5 wt % **HS-5-OH** in isostearyl alcohol gel	-	30.0, 18.8, 14.0, 5.9, 4.4, 4.0	31.7

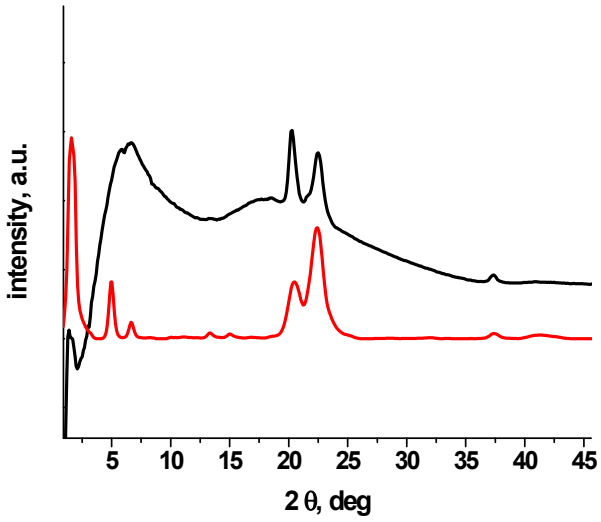

A

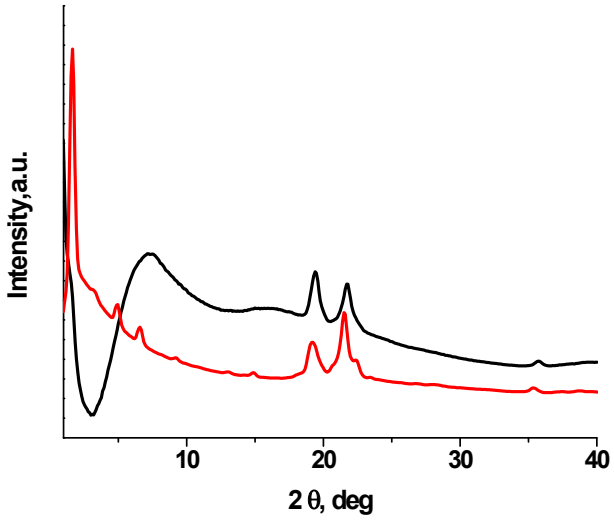

B

Figure S6. (A) XRD diffractograms at 22 °C of neat **HS-2-OH** (red) and its fast-cooled 5.0 wt % toluene gel (black). (B) XRD diffractograms at 24 °C of neat **HS-3-OH** (red) and its fast cooled 5 wt % **HS-3-OH** in toluene gel (black). The gel curves have been drawn after empirical subtraction of liquid component diffractions.

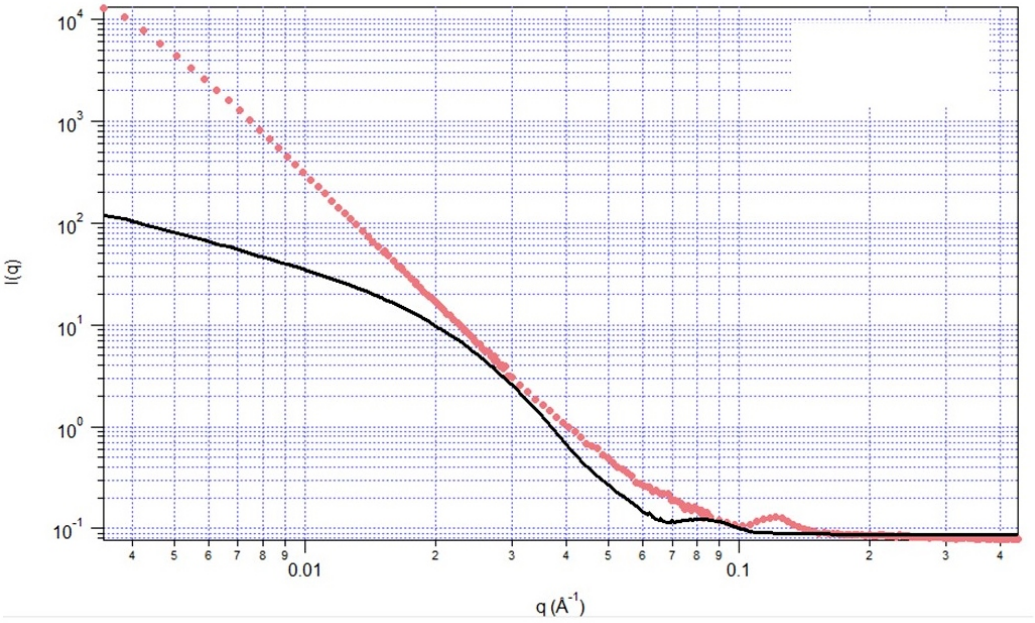

A

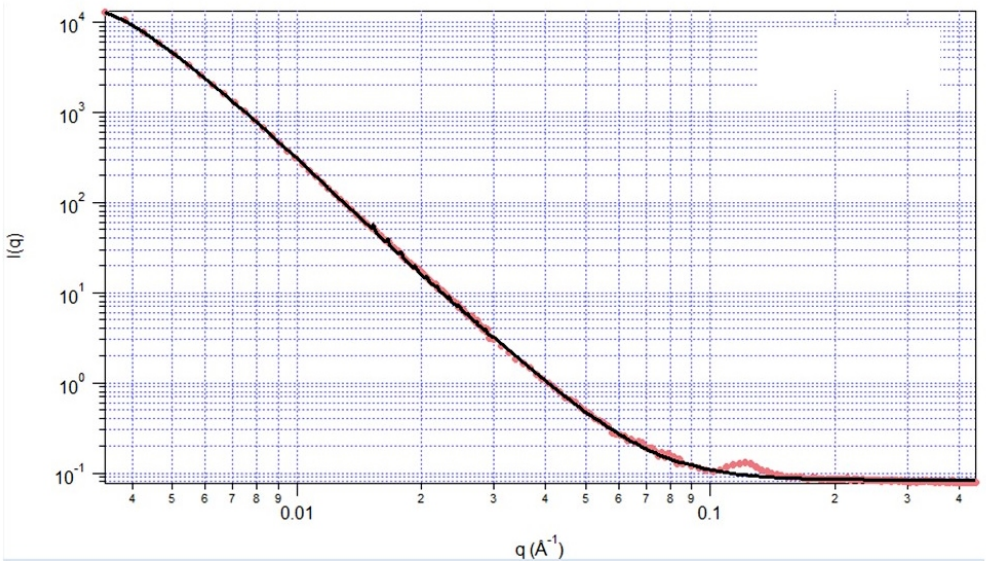

B

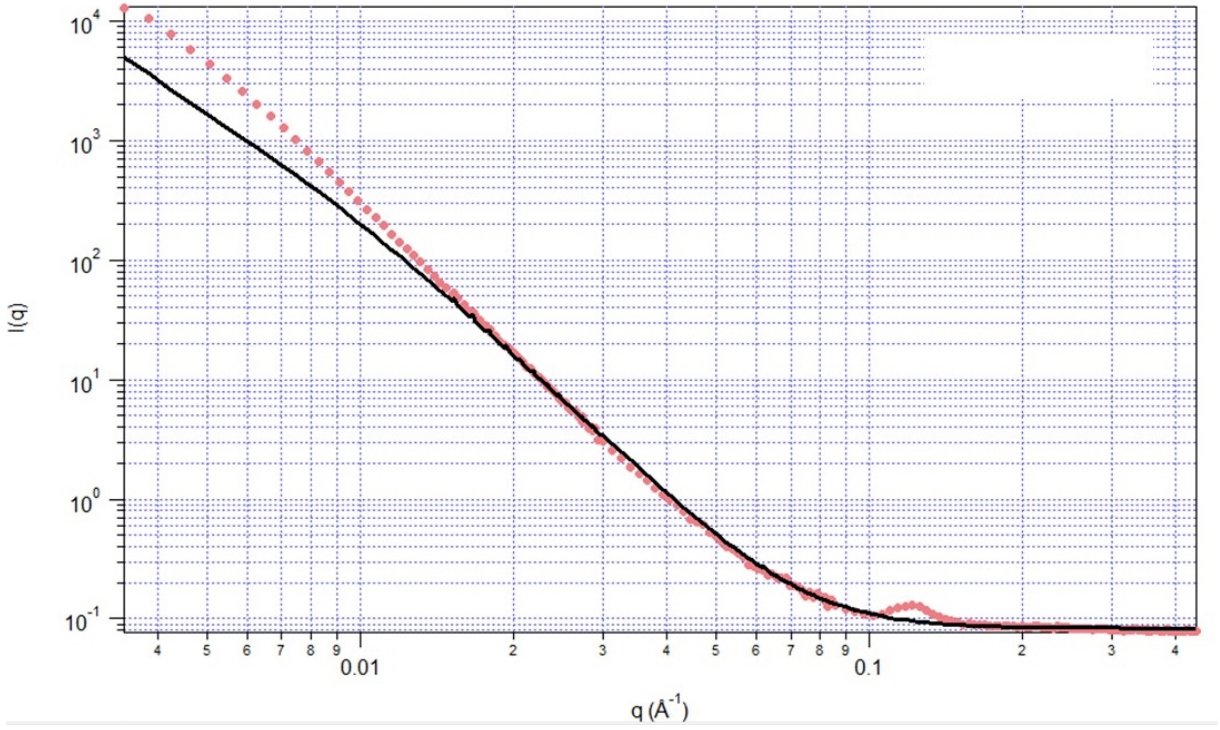

C

Figure S7. (A) SANS intensity (I) versus Q profile of a fast-cooled 2 wt % **HS-2-OH** in toluene-d_8 gel. (•) The black line is the theoretical curve obtained for fibers with parallelepiped cross-sections when no fitting constraints were imposed. (B) SANS intensity (I) versus Q profile of a fast-cooled

2 wt % **HS-2-OH** in a toluene-d_8 gel. (•) The black line is the theoretical curve for cylinders with contour length fixed at 1.1 x 10^4 Å; the fit obtained has radius 28.5 Å, Kuhn length 200 Å and polydispersity of radius 1.9. (C) SANS intensity (I) versus Q profile of a fast-cooled 2 wt % **HS-2-OH** in toluene-d_8 gel. (•) The black line is the theoretical curve for cylinders when the Kuhn length is fixed at 900 Å; the fit obtained has radius 28.0 Å, contour length 10^7 Å, and polydispersity of radius 1.9.

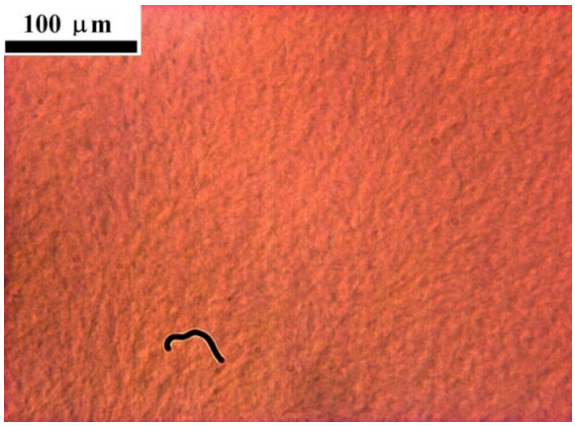

Figure S8. Polarizing optical micrograph at 23 °C of a 2 wt % **HS-2-OH** in toluene gel prepared by the fast-cooling protocol. The image was taken with a full-wave plate.

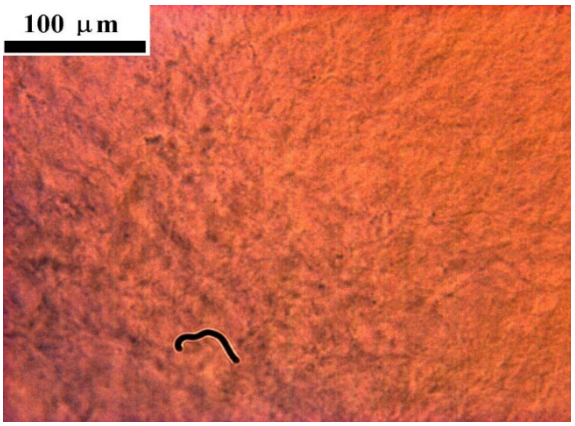

Figure S9. Polarizing optical micrograph at 23 °C of a 2 wt % **HS-2-OH** in toluene gel prepared by the slow-cooling protocol. The image was taken with a full-wave plate.

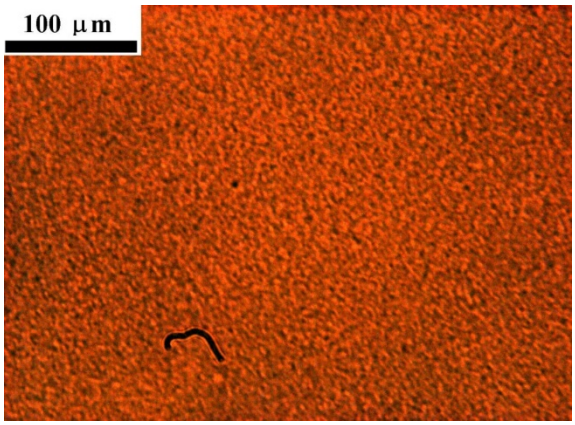

Figure S10. Polarizing optical micrograph at 23 °C of a 2 wt % **HS-2-OH** in silicone oil prepared by the fast-cooling protocol. The image was taken with a full-wave plate.

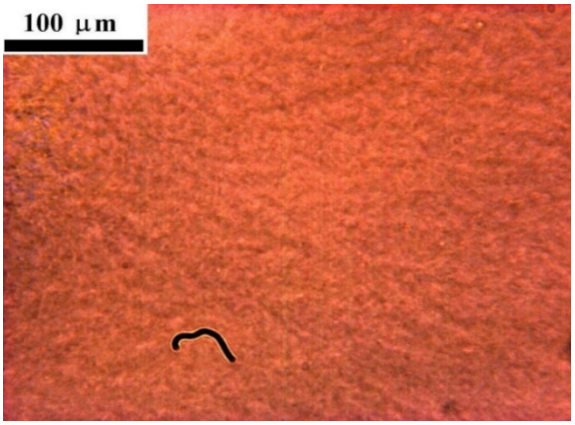

Figure S11. Polarizing optical micrograph at 23 °C of a 2 wt % silicone oil gel of **HS-2-OH** in silicone oil prepared by the slow-cooling protocol. The image was taken with a full-wave plate.

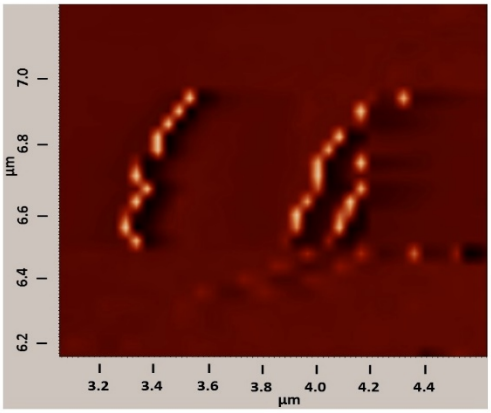

A

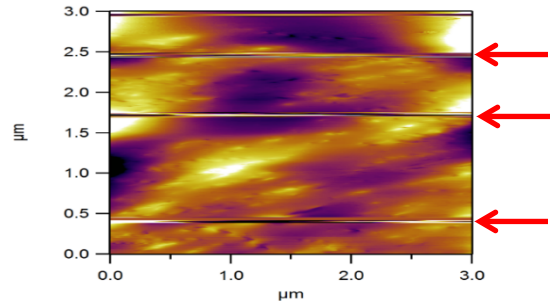

B

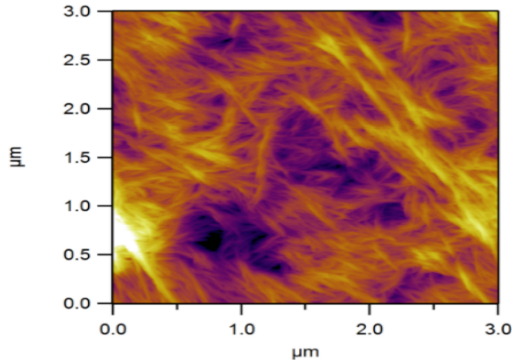

C

Figure S12 (A). AFM image of a fast-cooled 2 wt % **HS-2-OH** in isostearyl alcohol gel. (B) AFM image of a fast-cooled 2 wt % **HS-2-OH** in toluene gel. As the toluene was evaporating while images were being recorded, the distance between AFM tip and the surface changed significantly, resulting in the horizontal lines (shown with red arrows). At these times, the AFM tip was manually lowered towards the surface to maintain tracking. (C) AFM image of a fast-cooled 2 wt % **HS-2-OH** in toluene gel after most of the toluene was observed to have evaporated.

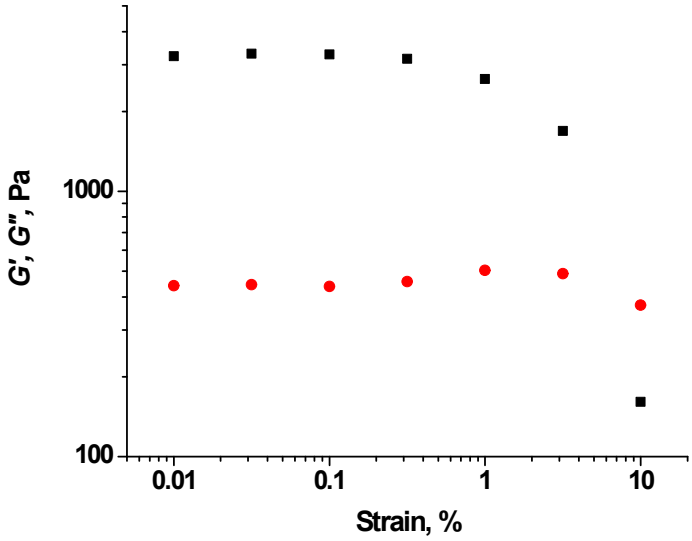

Figure S13. Log-log strain sweep (1.0 rad/sec) at 25 °C for a fast-cooled 2.0 wt % **HS-2-OH** in isostearyl alcohol gel: *G'*, black squares; *G''*, red circles.

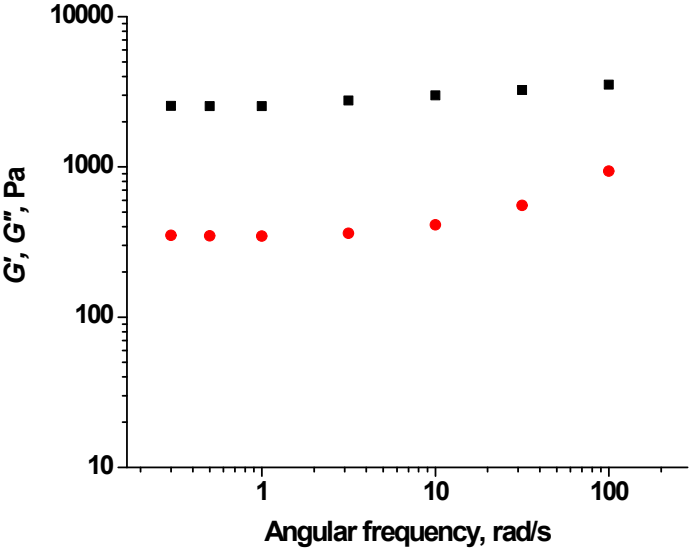

Figure S14. Log-log frequency sweep (0.05 % strain) at 25 °C for a fast-cooled 2 wt % **HS-2-OH** in isostearyl alcohol gel: *G'*, black squares; *G''*, red circles.

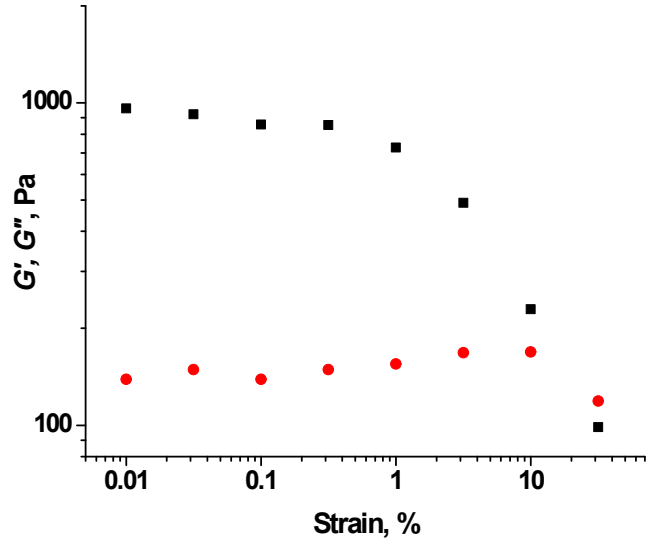

Figure S15. Log-log strain sweep (1.0 rad/sec) at 25 °C for a 2.0 wt % fast-cooled **HS-3-OH** in isostearyl alcohol gel: *G'*, black squares; *G''*, red circles.

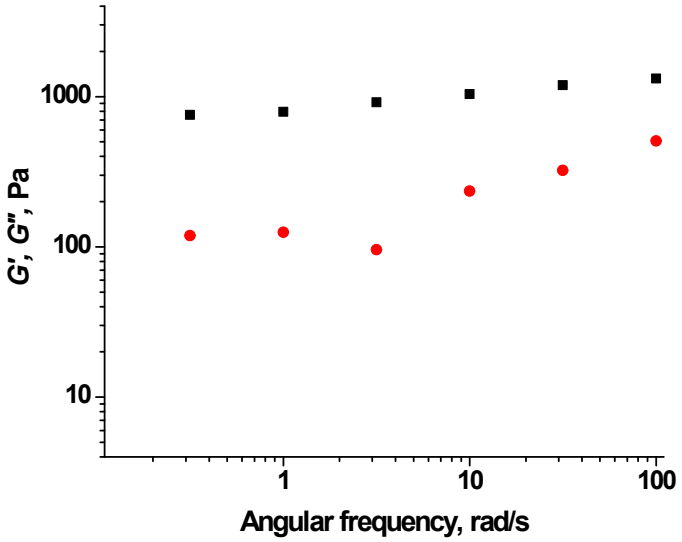

Figure S16. Log-log frequency sweep (0.05 % strain) at 25 °C for a fast-cooled 2.0 wt % **HS-3-OH** in isostearyl alcohol gel: *G'*, black squares; *G''*, red circles.

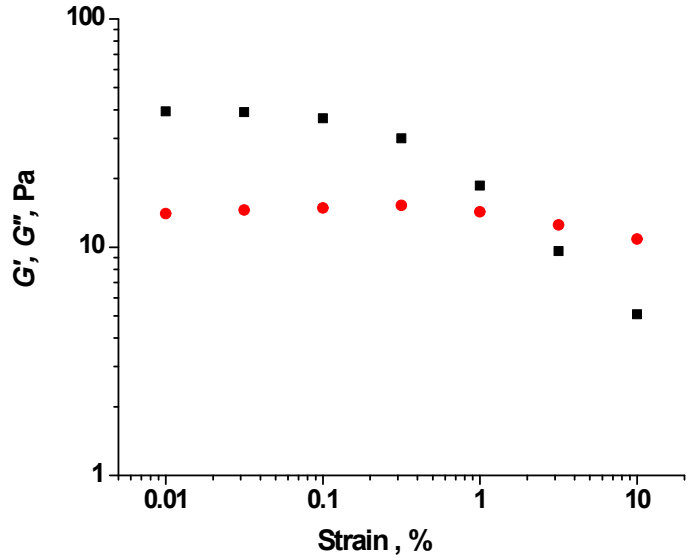

Figure S17. Log-log strain sweep (1.0 rad/sec) at 25 °C for a 2.0 wt % fast-cooled **HS-4-OH** in isostearyl alcohol gel: *G'*, black squares; *G''*, red circles.

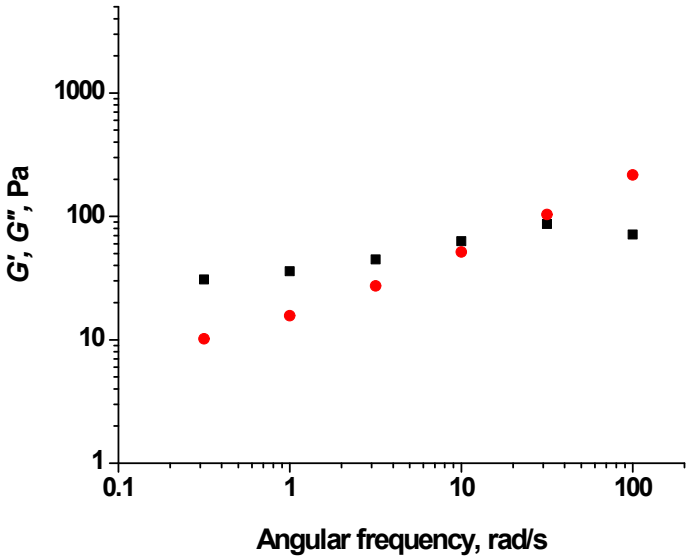

Figure S18. Log-log frequency sweep (0.05 % strain) at 25 °C for a 2 wt % fast-cooled **HS-4-OH** in isostearyl alcohol gel: *G'*, black squares; *G''*, red circles.

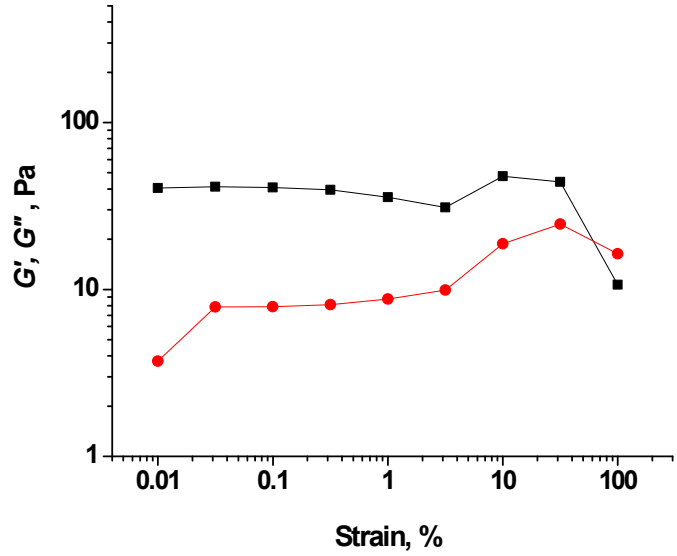

A

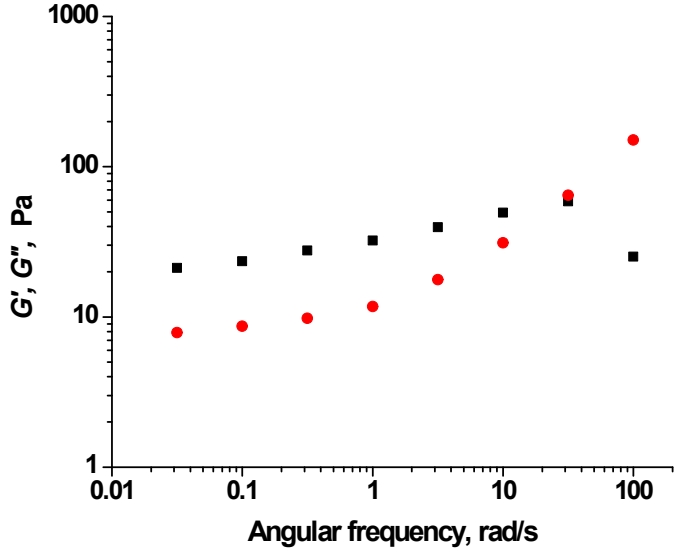

B

Figure S19. (A) Log-log strain sweep (1.0 rad/sec) at 25 °C for a 2.0 wt % fast-cooled **HS-5-OH** in isostearyl alcohol gel: *G'*, black squares; *G''*, red circles. (B) Log-log frequency sweep (0.05 % strain) at 25 °C for a 2 wt % fast-cooled **HS-5-OH** in isostearyl alcohol gel: *G'*, black squares; *G''*, red squares.

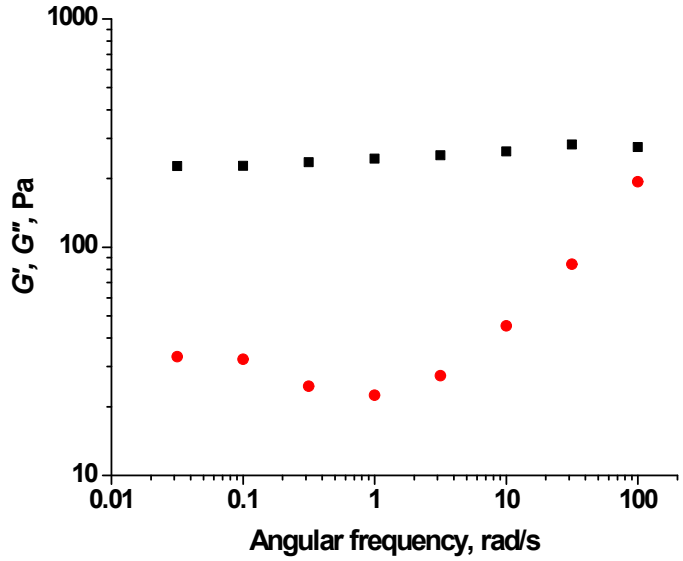

Figure S20. Log-log frequency sweep (0.05 % strain) at 25 °C for a 2 wt % **S-3-OH** in isostearyl alcohol gel: *G'*, black squares; *G''*, red circles.

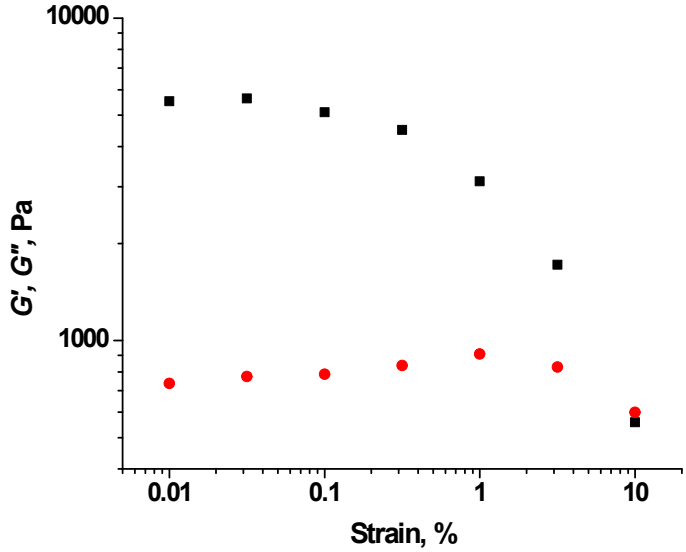

Figure S21. Log-log strain sweep (1.0 rad/sec) at 25 °C for a fast-cooled 2.0 wt % **HS-2-OH** in silicone oil gel: *G'*, black squares; *G''*, red circles.

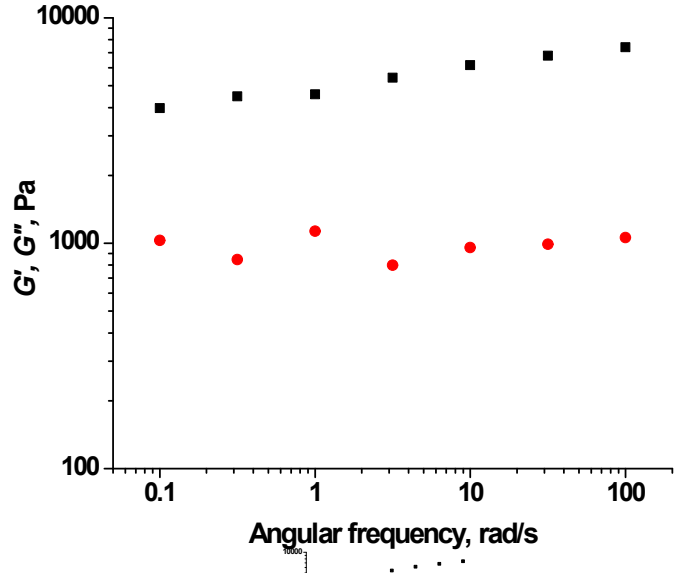

Figure S22. Log-log frequency sweep (0.05 % strain) at 25 °C for a fast-cooled 2.0 wt % **HS-2-OH** in silicone oil gel: *G'*, black squares; *G''*, red circles.

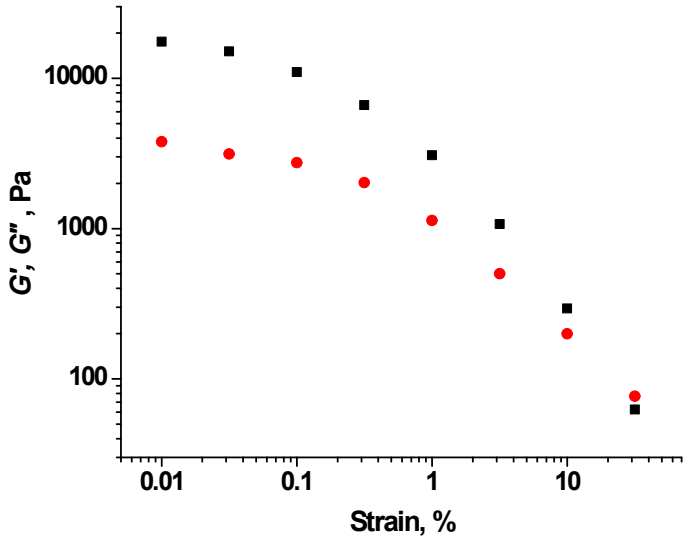

Figure S23. Log-log strain sweep (1.0 rad/sec) at 25 °C for a fast-cooled 2.0 wt % **HS-3-OH** in silicone oil gel: *G'*, black squares; *G''*, red circles.

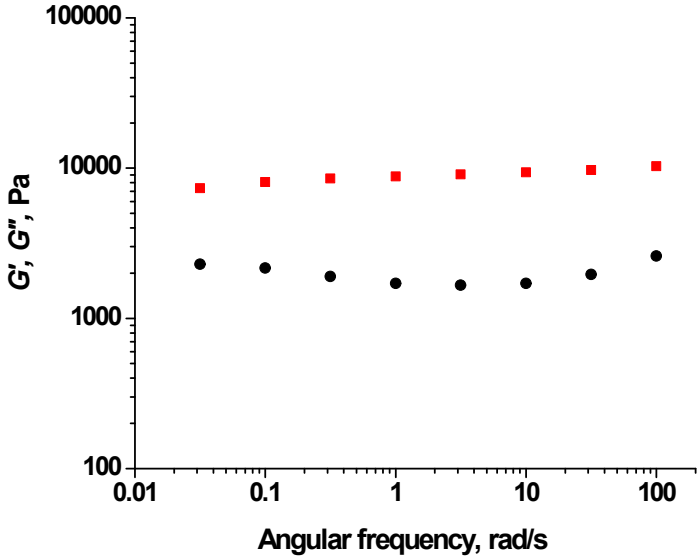

Figure S24. Log-log frequency sweep (0.05 % strain) at 25 °C for a fast-cooled 2.0 wt % **HS-3-OH** in silicone oil gel: *G'*, black squares; *G''*, red circles.

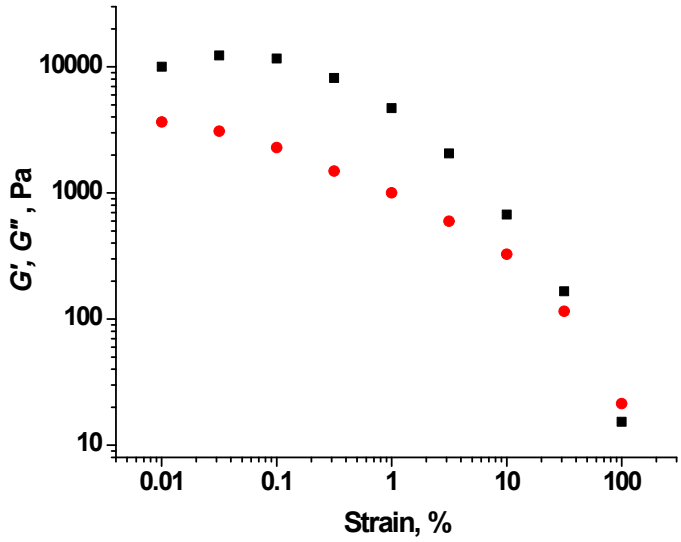

Figure S25. Log-log strain sweep (1.0 rad/sec) at 25 °C for a fast-cooled 2.0 wt % **HS-4-OH** in silicone oil gel: *G'*, black squares; *G''*, red circles.

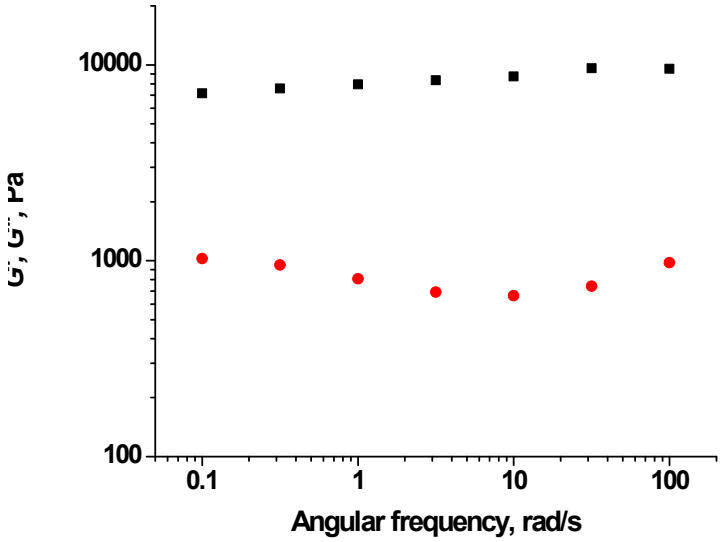

Figure S26. Log-log frequency sweep (0.05 % strain) at 25 °C for a fast-cooled 2.0 wt % **HS-4-OH** in silicone oil gel: *G'*, black squares; *G''*, red circles.

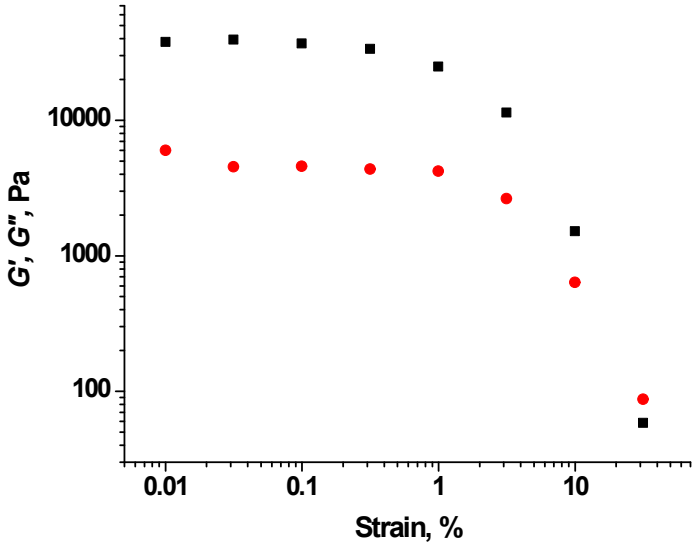

A

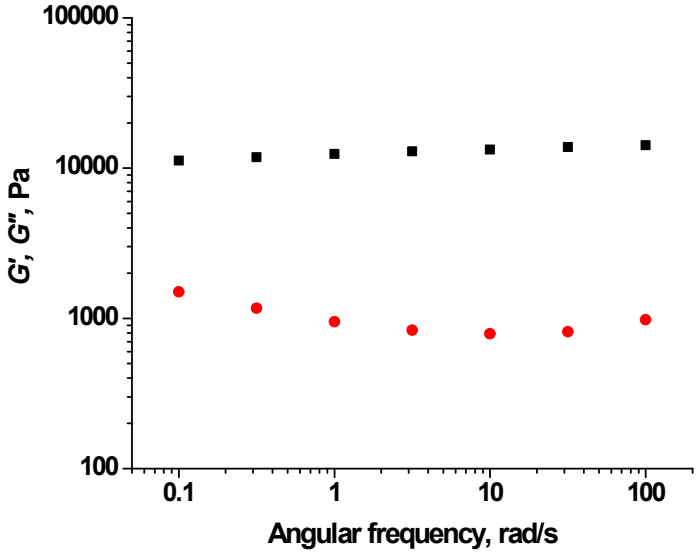

B

Figure S27. (A) Log-log strain sweep (1.0 rad/sec) at 25 °C for a fast-cooled 2.0 wt % **HS-4-OH** in silicone oil gel: *G'*, black squares; *G''*, red circles. (B) Log-log frequency sweep (0.05 % strain) at 25 °C for a fast-cooled 2.0 wt % **HS-5-OH** in silicone oil gel: *G'*, black squares; *G''*, red circles.

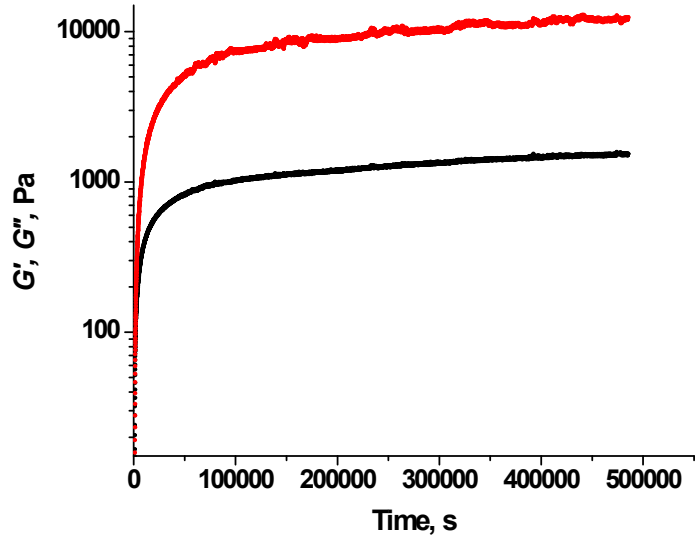

Figure S28. Plots of *G'* (red) and *G''* (black) versus time for a 2 wt % **HS-2-OH** in isostearyl alcohol gel sample starting immediately upon reaching 25 °C after its sol was cooled from 110 °C over ca. 5 min; 0.05 % strain and 1 rad/sec angular frequency.

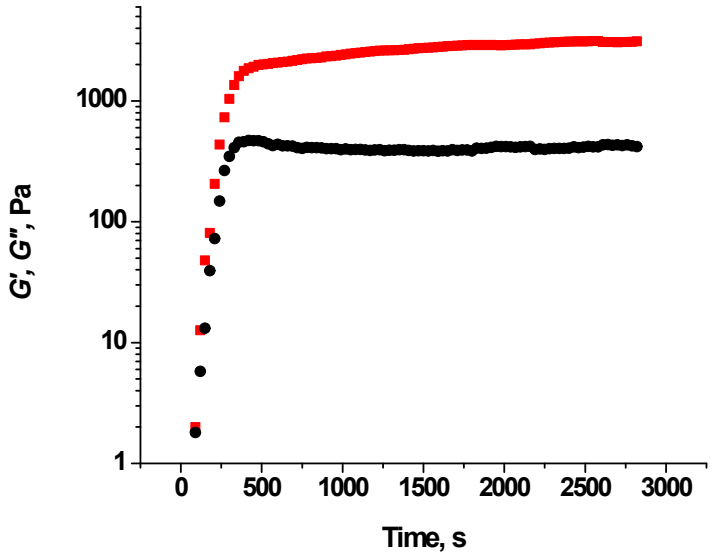

Figure S29. Plots of *G'* (red) and *G"* (black) versus time for a 2 wt % **HS-3-OH** in isostearyl alcohol gel sample starting immediately upon reaching 25 °C after its sol was cooled from 110 °C over ca. 5 min; 0.05 % strain and 1 rad/sec angular frequency.

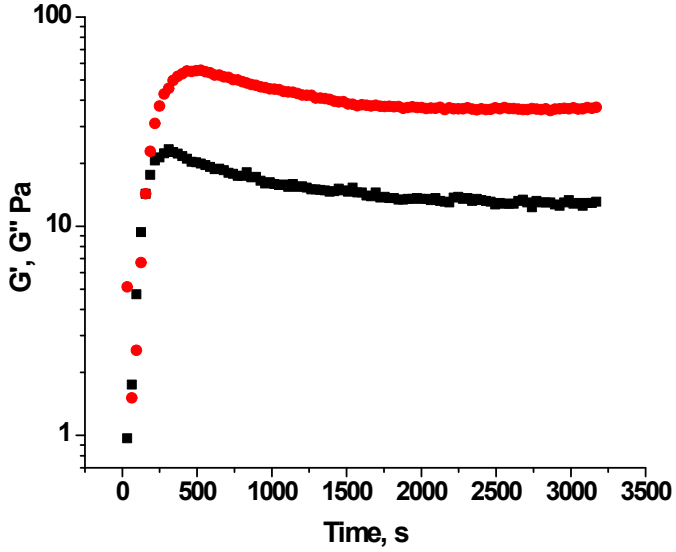

Figure S30. Plots of *G'* (red) and *G"* (black) versus time for a 2 wt % **HS-4-OH** in isostearyl alcohol gel sample starting immediately upon reaching 25 °C after its sol was cooled from 110 °C over ca. 5 min; 0.05 % strain and 1 rad/sec angular frequency.

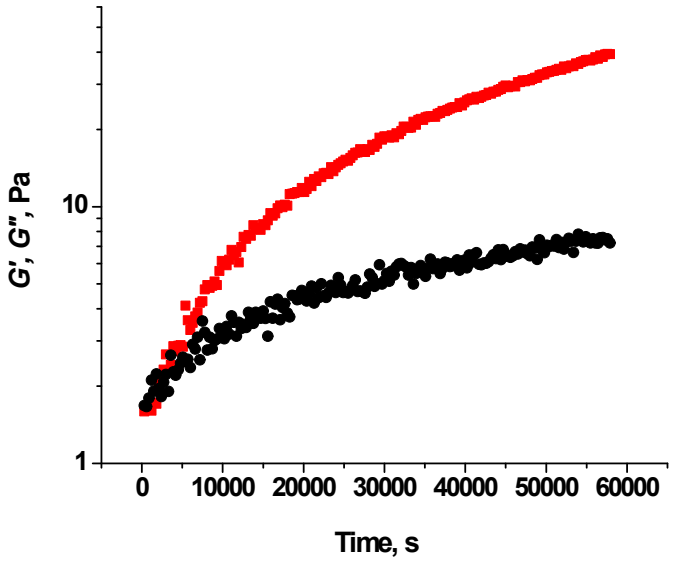

Figure S31. Plots of *G'* (red) and *G"* (black) versus time for a 2 wt % **HS-5-OH** in isostearyl alcohol gel sample starting immediately upon reaching 25 °C after its sol was cooled from 110 °C over ca. 5 min; 0.05 % strain and 1 rad/sec angular frequency.

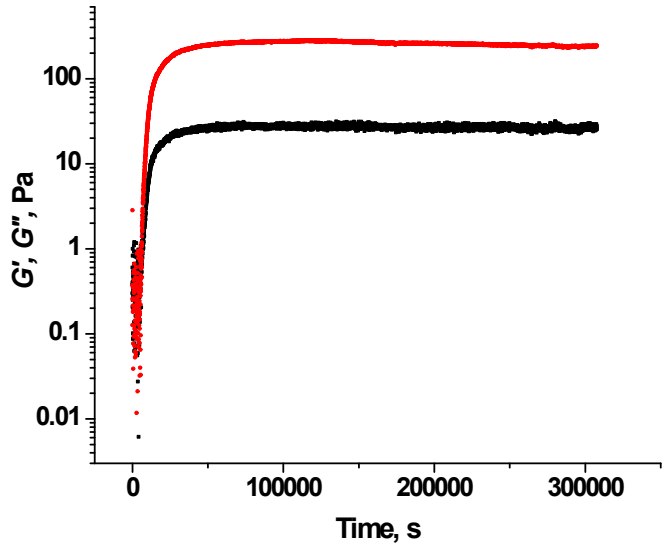

A

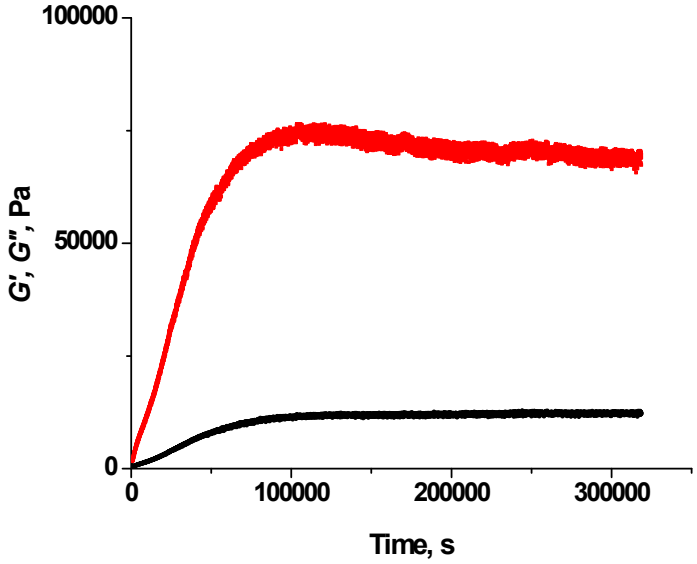

B

Figure S32. Plots of *G'* (red) and *G"* (black) versus time for gels consisting of (A) 2 wt % **S-3-OH** in isostearyl alcohol gel and (B) **HS-3** in isostearyl alcohol gels. Measurements commenced immediately upon reaching 25 °C after the sols were cooled from 110 °C over ca. 5 min; 0.05 % strain and 1 rad/sec angular frequency.

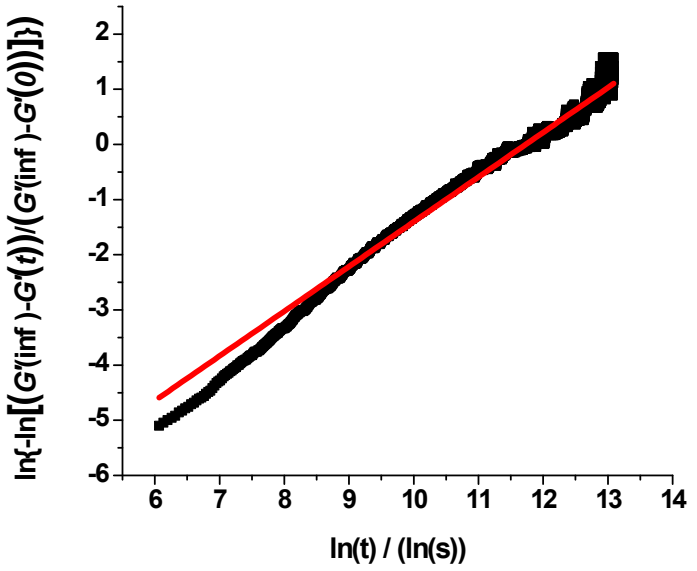

Figure S33. Linear fits to the Avrami equation 1 (main text) of *G'* from kinetic rheology data in Figure S28; slope = 0.85 (R^2 = 0.97).

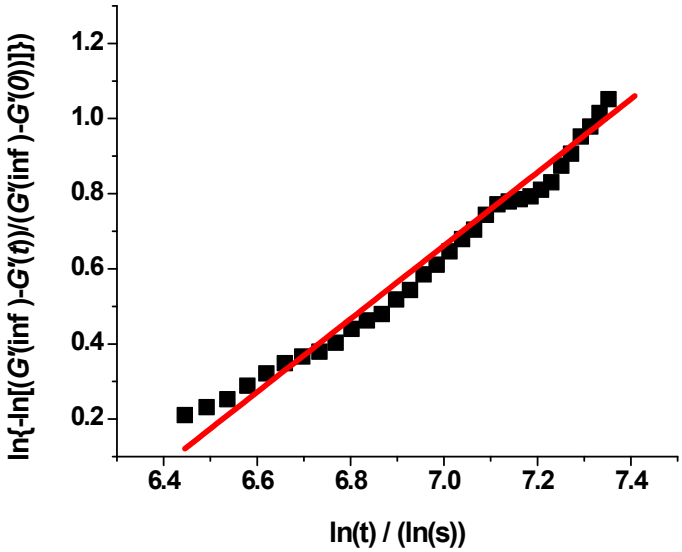

Figure S34. Linear fits to the Avrami equation 1 (main text) of *G'* from kinetic rheology data in Figure S29: slope = 0.98 (R^2 = 0.98).

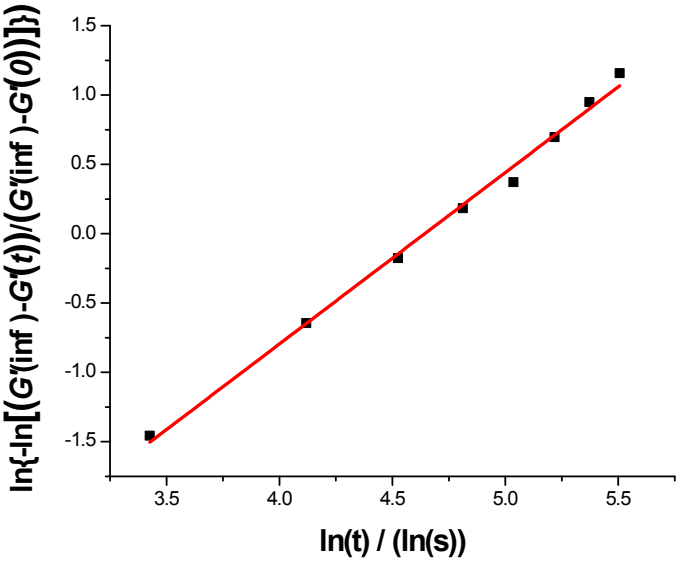

Figure S35. Linear fits to the Avrami equation 1 (main text) of *G'* from kinetic rheology data in Figure S30; slope = 1.2 (R^2 = 0.97).

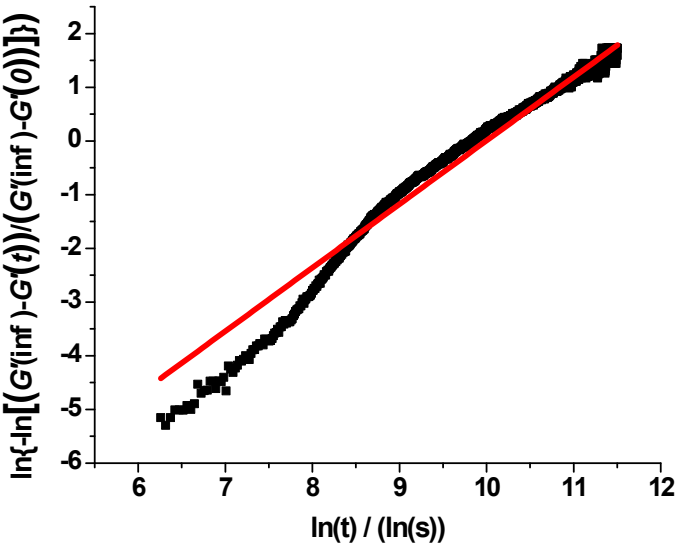

A

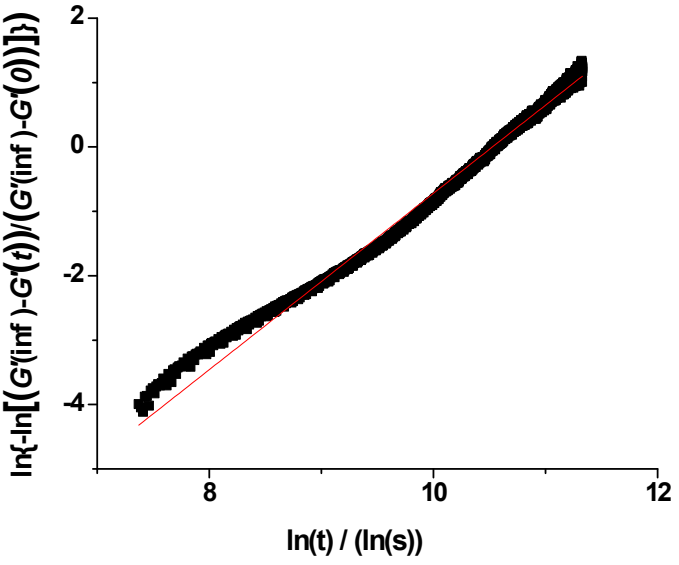

B

Figure 36. Linear fits to the Avrami equation 1 (main text) of *G'* (A) from kinetic rheology data in Figure S32A; slope = 1.1 (R^2 = 0.97) and (B) from kinetic rheology data in Figure S32B; slope = 1.4 (R^2 = 0.99).

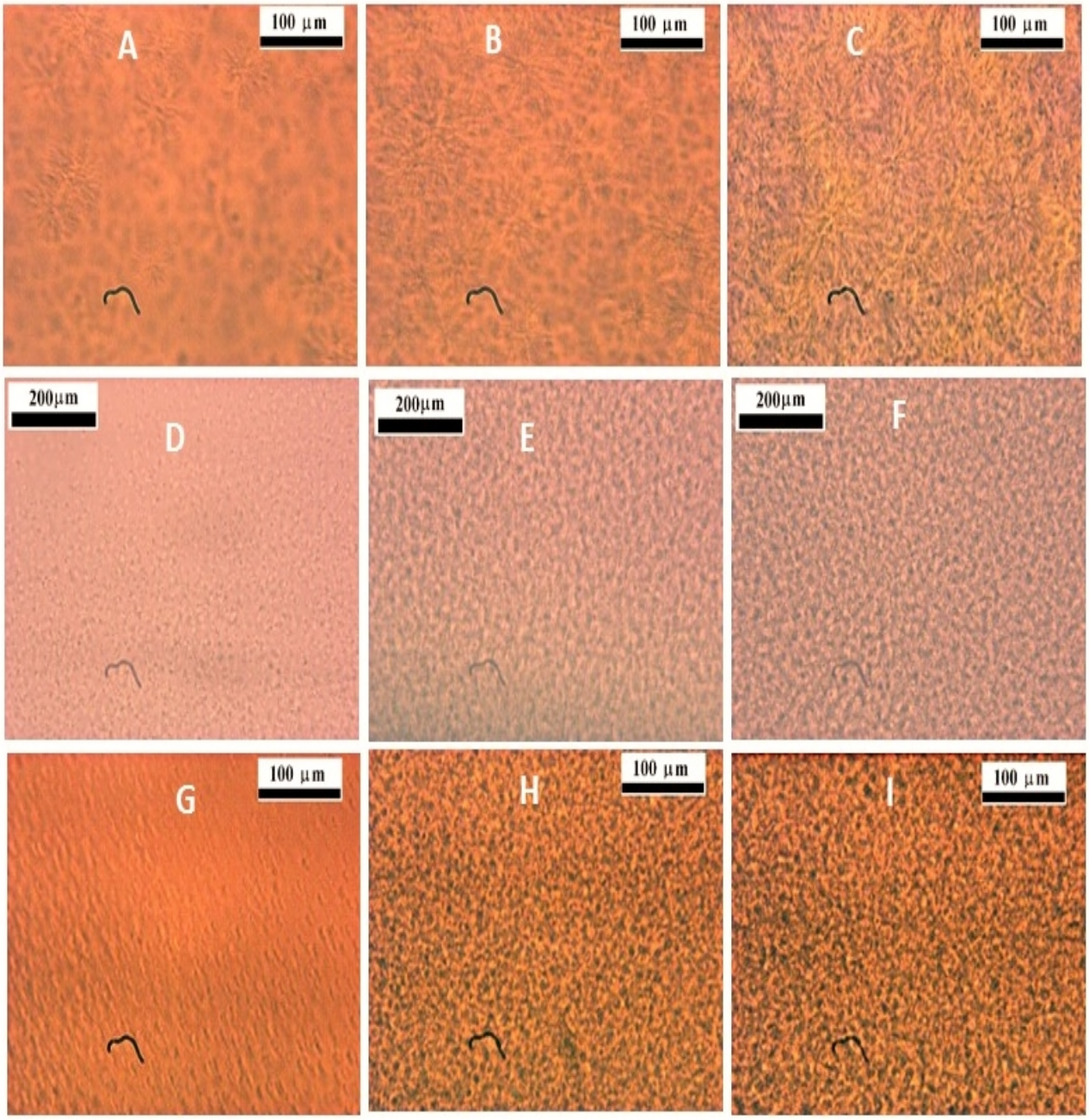

Figure S37. POM images at 25°C of a 2 wt % **HS-n-OH** in isostearyl alcohol sol at different times after being fast-cooled from 110 to 25 °C (at ~20 °C/min): (A) **HS-3-OH** in isostearyl alcohol at 1 min; (B) **HS-3-OH** in isostearyl alcohol at 2 min ; (C) **HS-3-OH** in isostearyl alcohol at 15 min; (D) **HS-4-OH** in isostearyl alcohol at 1 min; (E) **HS-4-OH** in isostearyl alcohol at 3 min; (F) **HS-4-OH** in isostearyl alcohol at 60 min; (G) **HS-5-OH** in isostearyl alcohol at 45 min; (H) **HS-5-OH** in isostearyl alcohol at 60 min; (I) **HS-5-OH** in isostearyl alcohol at 150 min. The images were taken with a full-wave plate.

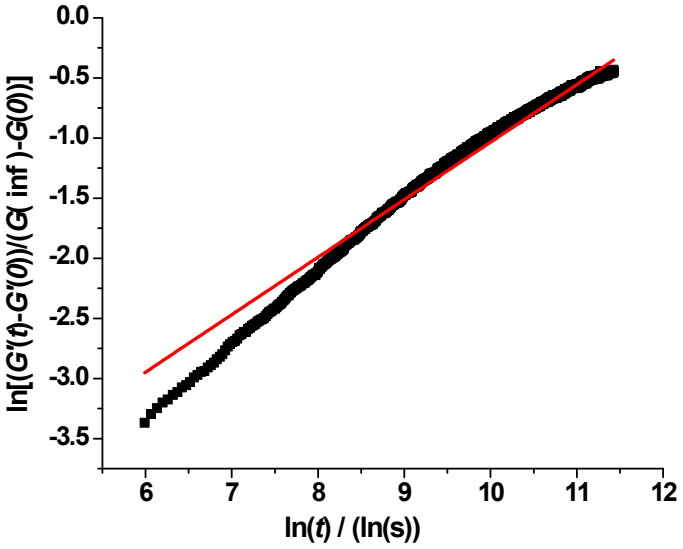

Figure S38. Linear fits to the Dickinson equation 2 (main text) of *G'* from kinetic rheology data in Figure S28; slope = 0.48, D_f = 2.02, (R^2 = 0.98).

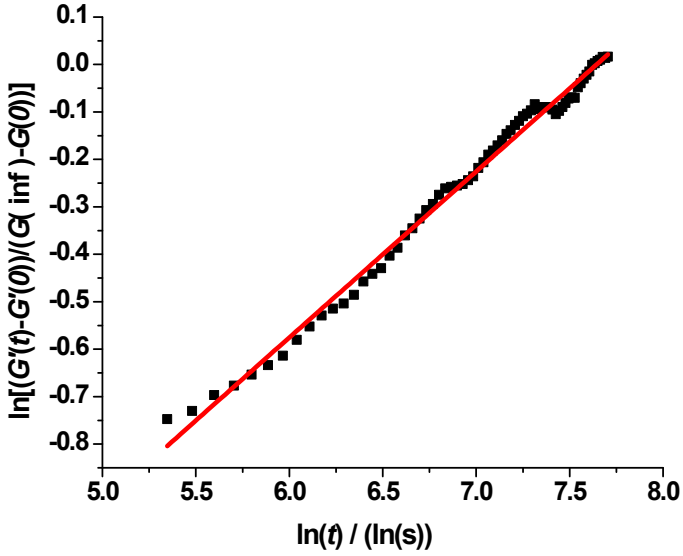

Figure S39. Linear fits to the Dickinson equation 2 (main text) of *G'* from kinetic rheology data in Figure S29; slope = 0.35, D_f = 2.22, (R^2 = 0.99).

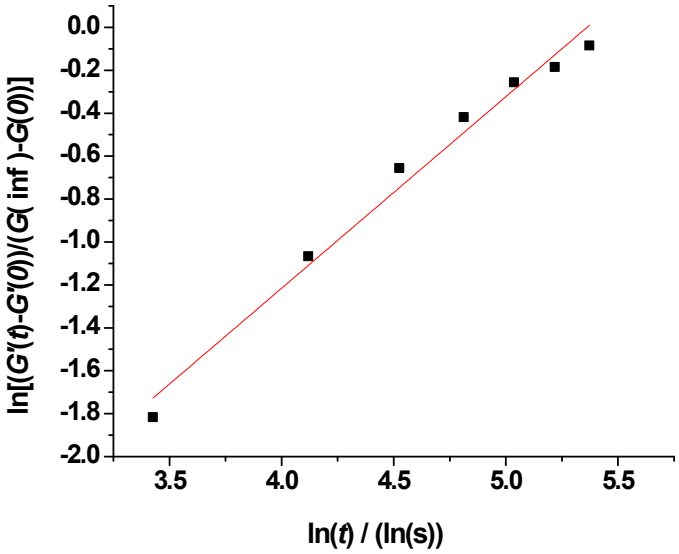

Figure S40. Linear fits to the Dickinson equation 2 (main text) of *G'* from kinetic rheology data in Figure S30; slope = 0.89, D_f = 1.6, (R^2 = 0.99).

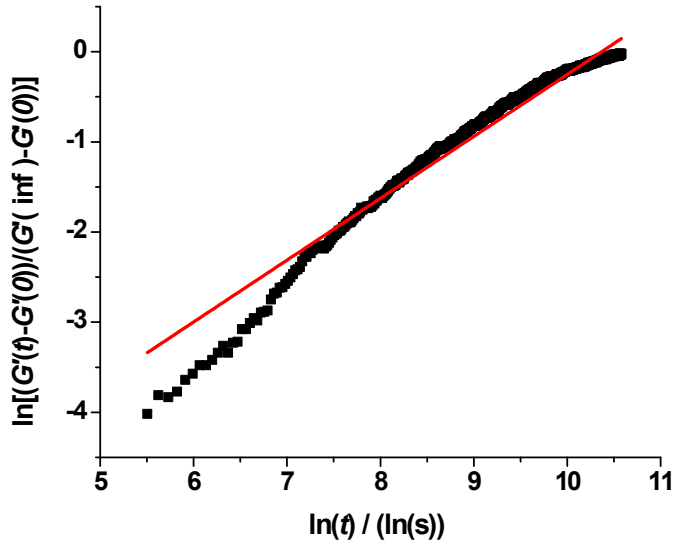

A

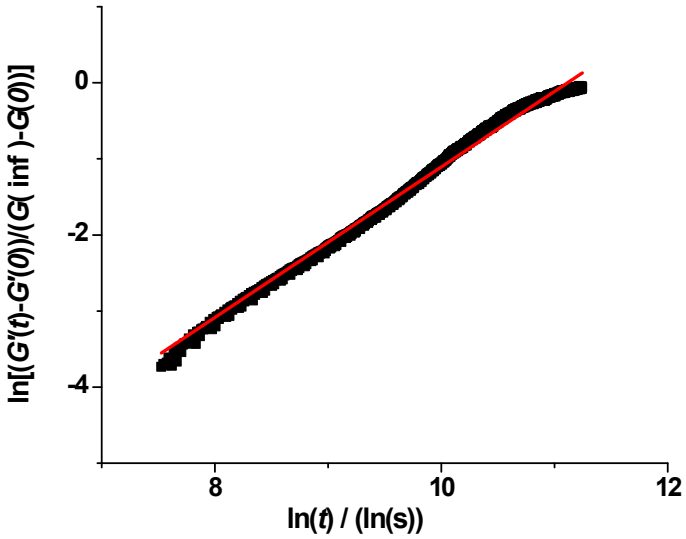

B

Figure S41. Linear fits to the Dickinson equation 2 (main text) of *G'* (A) from kinetic rheology data in Figure S32A; slope = 0.6, D_f = 1.9, (R^2 = 0.96) and (B) from kinetic rheology data in Figure S32B; slope = 0.6, D_f = 1.9, (R^2 = 0.96).

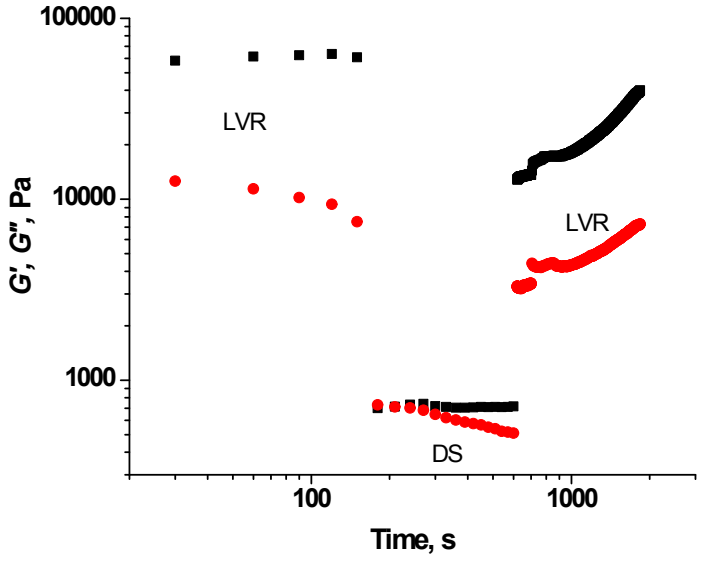

A

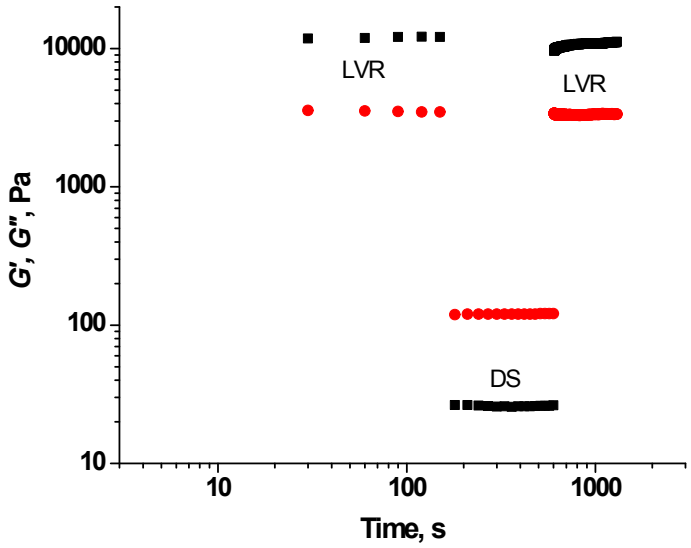

B

Figure 42. A) *G'* (●) and *G"* (■) at 25 ºC as a function of time and application of different strains and frequencies to a fast-cooled 2 wt % **HS-2-OH** in toluene gel. Linear viscoelastic region (LVR): γ = 0.03 %, ω = 100 rad/s. Destructive strain (DS): γ = 50 %, ω = 1 rad/s. Rotational strain was kept at 0 % for 0.05 s before changing from DS to LVR conditions. A second cycle was not run because of noticeable evaporation of the toluene over protracted periods, even though a solvent trap was employed. B) *G'* (●) and *G"* (■) at 25 ºC as a function of time and application of different strains and frequencies to a fast-cooled 2 wt % **HS-2-OH** in silicone oil gel. Linear viscoelastic region (LVR): γ = 0.1 %, ω = 100 rad/s. Destructive strain (DS): γ = 30 %, ω = 1 rad/s. Rotational strain was kept at 0 % for 0.05 s before changing from DS to LVR conditions. The *G'* recovery after a second cycle was >99%.

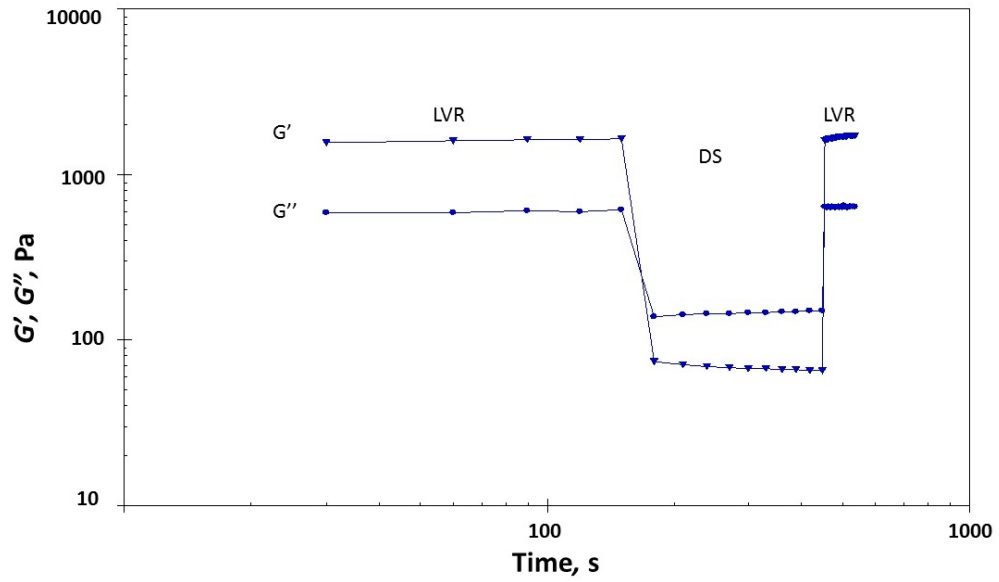

Figure S43. *G'* (▼) and *G''* (■) at 25 ºC as a function of time and application of different strains and frequencies to a fast-cooled 2.0 wt % **HS-3-OH** in isostearyl alcohol gel. Linear viscoelastic region (LVR): γ = 0.05 %, ω = 100 rad/s. Destructive strain (DS): γ = 30 %, ω = 1 rad/s. Rotational strain was kept at 0 % for 0.05 s before changing from DS to LVR conditions.

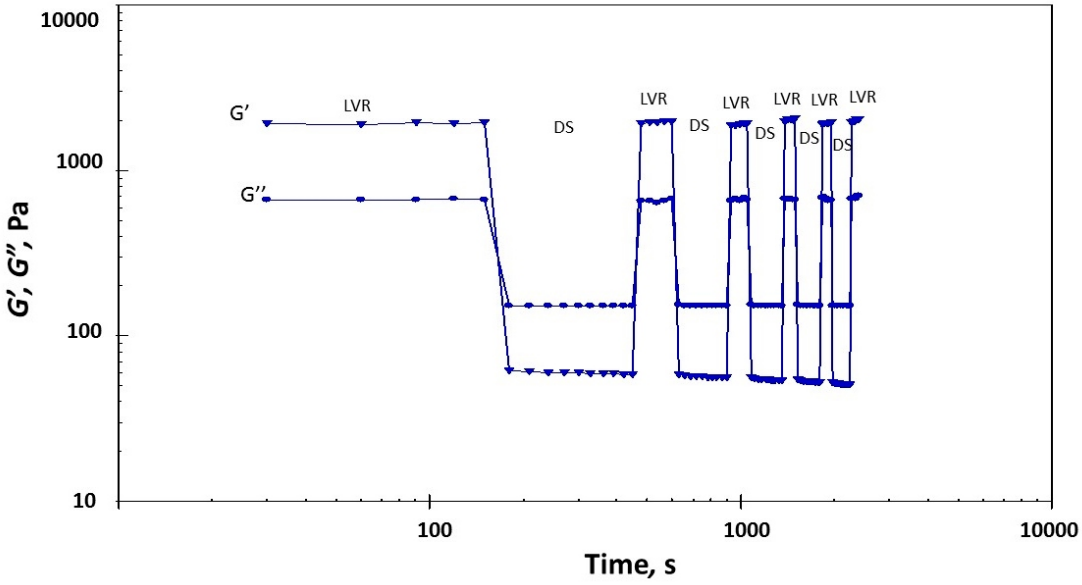

Figure S44. *G'* (▼) and *G''* (■) at 25 ºC as a function of time and application of different strains and frequencies to a fast-cooled 2.0 wt % **HS-3-OH** in isostearyl alcohol gel. Linear viscoelastic region (LVR): γ = 0.05 %, ω = 100 rad/s. Destructive strain (DS): γ = 30 %, ω = 1 rad/s. Rotational strain was kept at 0 % for 0.05 s before changing from DS to LVR conditions.

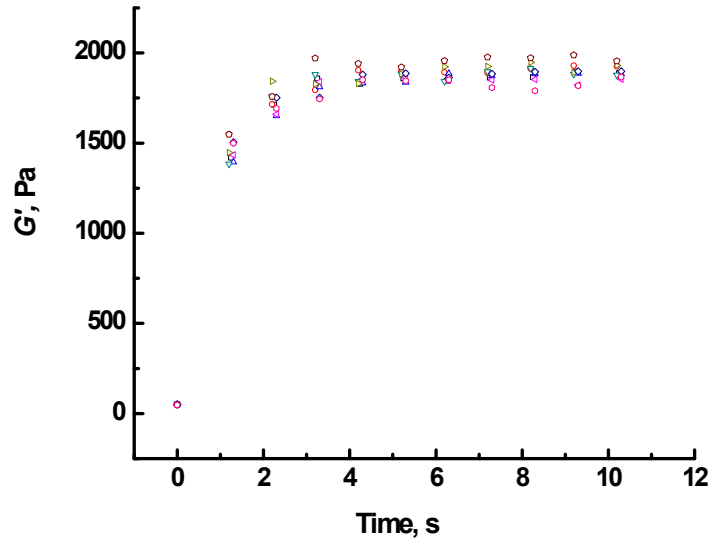

Figure S45. Recovery of *G*' versus time after cessation of destructive strain (using data from Figure 5) of a fast-cooled 2.0 wt % **HS-3-OH** in isostearyl alcohol gel at 25 ºC recorded in the linear viscoelastic regime (LVR, γ = 0.05 %, ω = 100 rad/s).

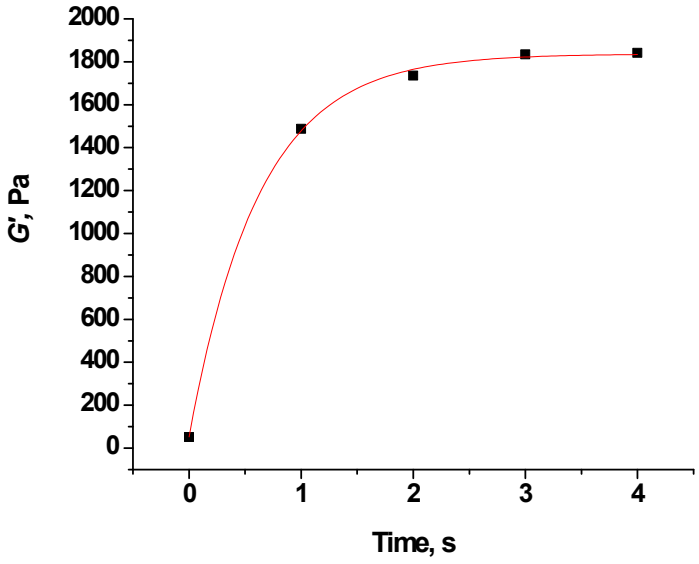

Figure S46. Recovery of *G*' (average of 10 consecutive thixotropic recovery cycles, Figure 5) of a fast-cooled 2.0 wt % **HS-3-OH** in isostearyl alcohol gel at 25 ºC recorded in the linear viscoelastic regime (LVR, γ = 0.05 %, ω = 100 rad/s) after applying a destructive strain (γ = 30 %, ω = 1 rad/s; rotational strain was kept at 0 % for 0.05 s) and best single exponential rise fit (red line) according to eq 3 in the main text. (τ = 0.62 ± 0.03 s (R^2 = 0.999)).

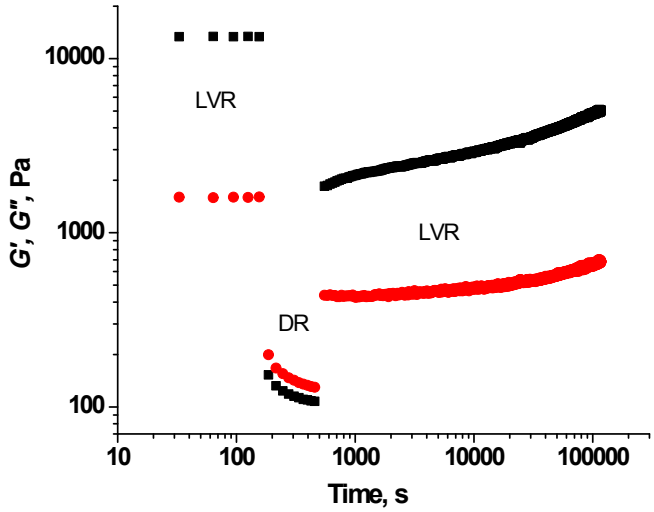

Figure S47. *G'* (■) and *G''* (●) at 25 ºC as a function of time and application of different strains and frequencies to a fast-cooled 2.0 wt % **HS-2-OH** in isostearyl alcohol gel. Linear viscoelastic region (LVR): strain = 0.05 %, ω = 100 rad/s. Destructive strain (DS): strain = 30 %, ω = 1 rad/s. Rotational strain was kept at 0 % for 0.05 s before changing from DS to LVR conditions.

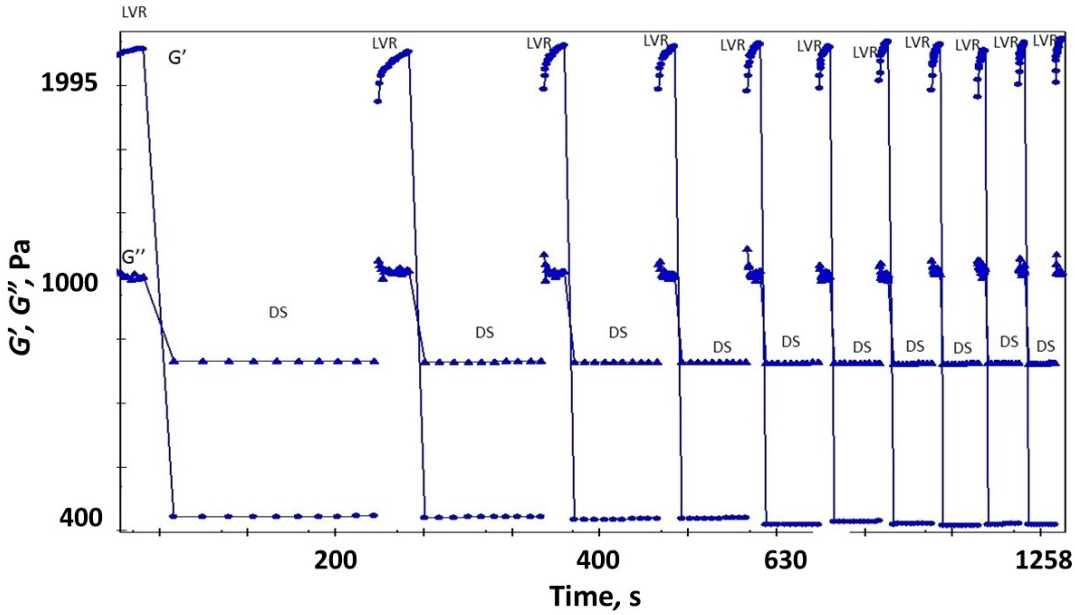

Figure S48. *G'* (●) *G''* (▲) at 25 ºC as a function of time and application of different strains and frequencies to a fast-cooled 2.0 wt % **HS-2-OH** in isostearyl alcohol gel obtained after the experiment described in Figure S45. Linear viscoelastic region (LVR): γ = 0.05 %, ω = 100 rad/s.

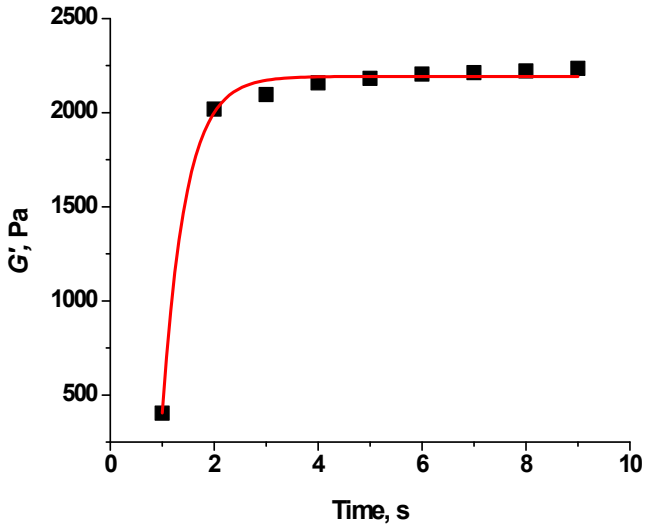

Figure S49. Recovery of *G'* (average of 9 consecutive thixotropic recovery measurements from Figure S48A) of a 2.0 wt % **HS-2-OH** in isostearyl alcohol gel (fast-cooled) at 25 ºC recorded at linear viscoelastic regime (LVR, γ = 0.05 %, ω = 100 rad/s) after applying a destructive strain (γ = 30 %, ω = 1 rad/s, rotational strain was kept at 0 % for 0.05 s) and best single exponential decay fit (red line) according to equation 3. (τ = 0.45 ± 0.05 s, R^2: 0.99).

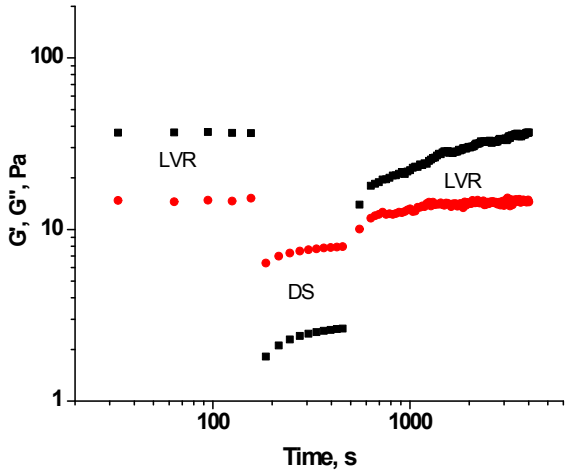

Figure S50. *G'* (■) and *G''* (●) at 25 ºC as a function of time and application of different strains and frequencies to a fast-cooled 2.0 wt % **HS-4-OH** in isostearyl alcohol gel. Linear viscoelastic region (LVR): strain = 0.05 %, ω = 100 rad/s. Destructive strain (DS): strain = 30 %, ω = 1 rad/s. Rotational strain was kept at 0 % for 0.05 s before changing from DS to LVR conditions.

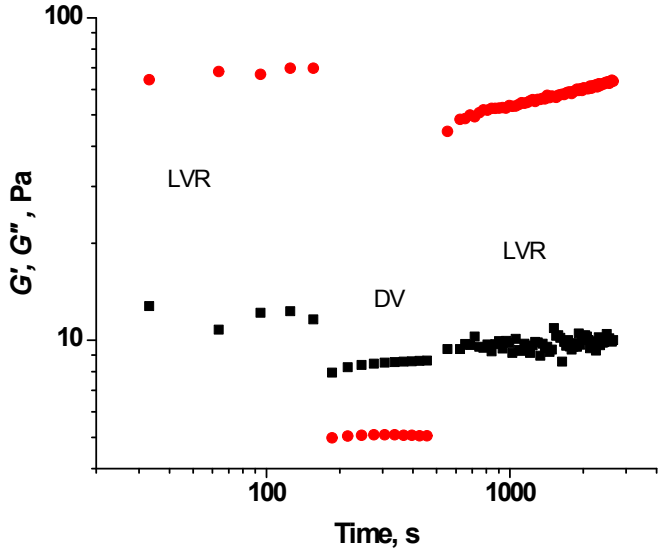

Figure 51. *G'* (●) and *G"* (■) at 25 ºC as a function of time and application of different strains and frequencies to a fast-cooled 2.0 wt % **HS-5-OH** in isostearyl alcohol gel. Linear viscoelastic region (LVR): γ = 0.05 %, ω = 100 rad/s. Destructive strain (DS): γ = 30 %, ω = 1 rad/s. Rotational strain was kept at 0 % for 0.05 s before changing from DS to LVR conditions.

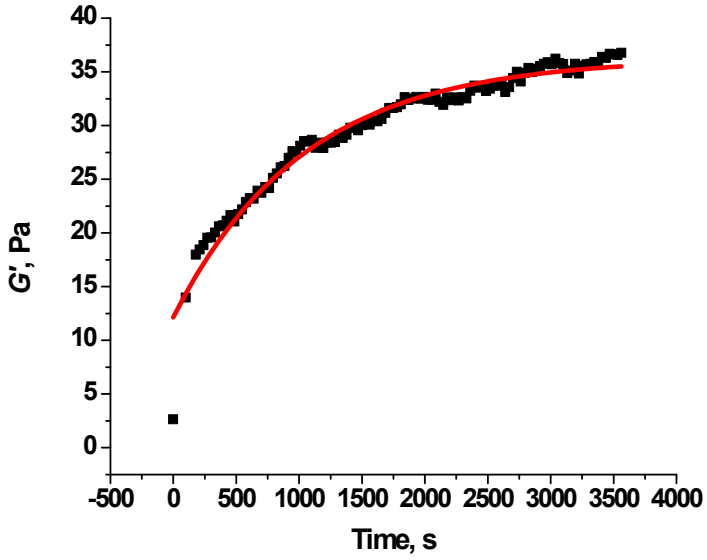

Figure S52. Recovery of *G*' of a 2.0 wt % **HS-4-OH** in isostearyl alcohol gel (fast-cooled) at 25 ºC recorded in the linear viscoelastic regime (LVR, strain = 0.05 %, ω = 100 rad/s) after applying a destructive strain (strain = 30 %, ω = 1 rad/s; rotational strain was kept at 0 % for 0.05 s) and best single exponential growth fit (red line) according to eq 3 in the main text.

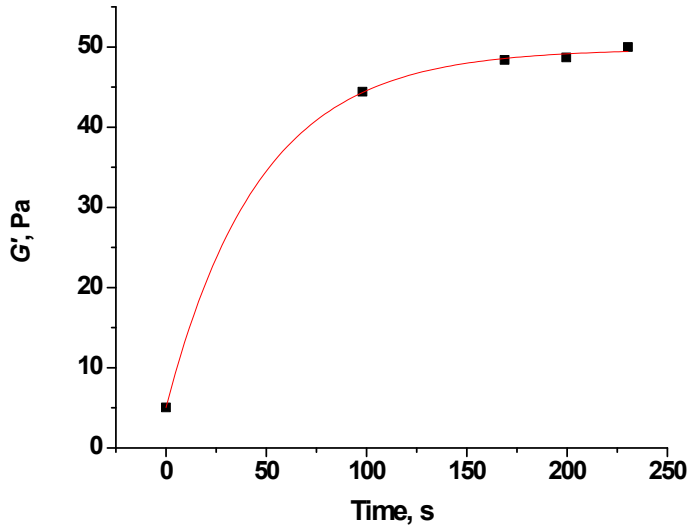

Figure S53. Recovery of *G'* of a 2.0 wt % **HS-5-OH** in isostearyl alcohol gel (fast-cooled) at 25 ºC recorded in the linear viscoelastic regime (LVR, strain = 0.05 %, ω = 100 rad/s) after applying a destructive strain (strain = 30 %, ω = 1 rad/s; rotational strain was kept at 0 % for 0.05 s) and best single exponential growth fit (red line) according to eq 3 in the main text.

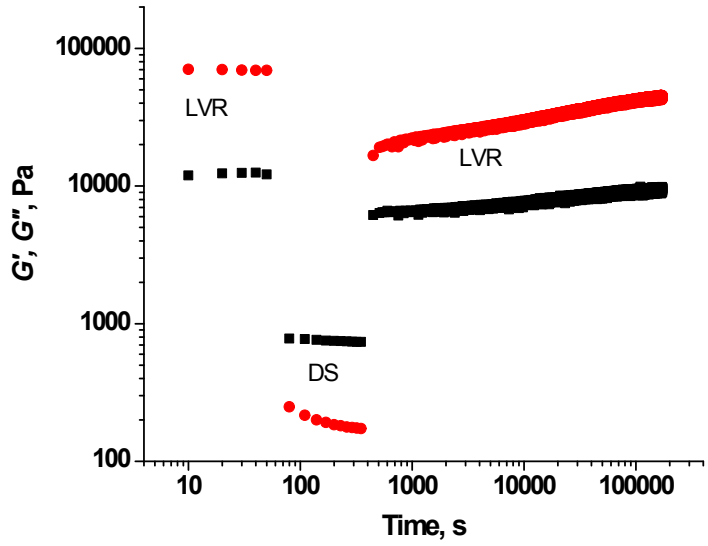

Figure 54. *G'* (●) and *G"* (■) at 25 ºC as a function of time and application of different strains and frequencies to a fast-cooled 2.0 wt % 2 wt % 12-hydroxy-N-propyloctadecanamide /isostearyl alcohol gel. Linear viscoelastic region (LVR): γ = 0.05 %, ω = 100 rad/s. Destructive strain (DS): γ = 30 %, ω = 1 rad/s. Rotational strain was kept at 0 % for 0.05 s before changing from DS to LVR conditions.

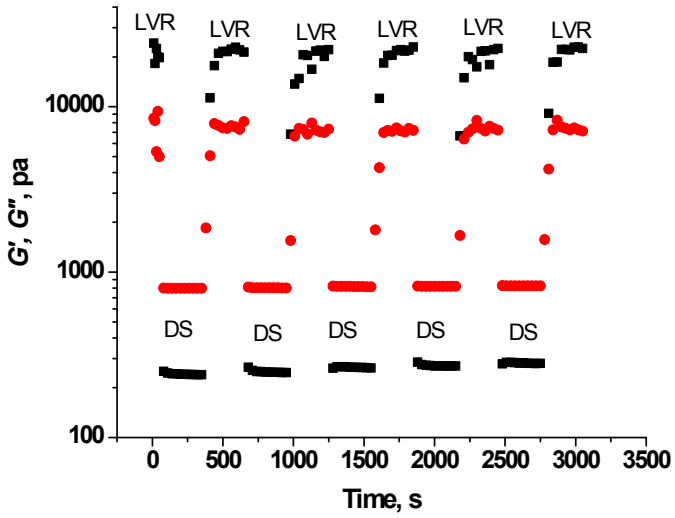

Figure S55. *G'* (black) and *G''* (red) at 25 ºC as a function of time and application of different strains and frequencies to a fast-cooled 2.0 wt % 12-hydroxy-N-propyloctadecanamide in isostearyl alcohol gel. Linear viscoelastic region (LVR): γ = 0.05 %, ω = 100 rad/s. Destructive strain (DS): γ = 30 %, ω = 1 rad/s. Rotational strain was kept at 0 % for 0.05 s before changing from DS to LVR conditions.

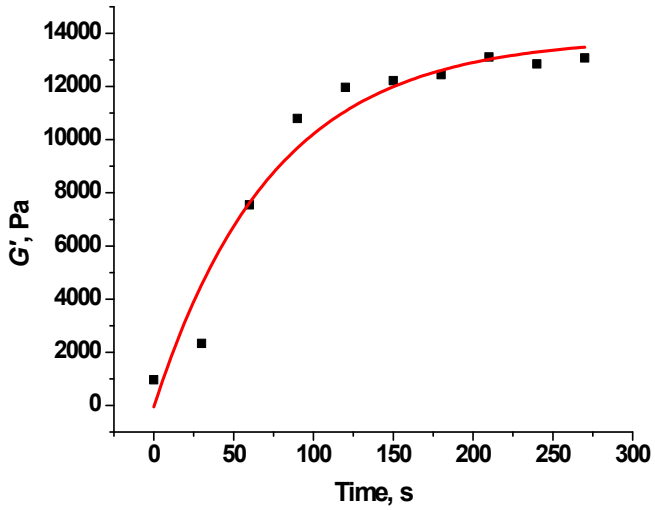

Figure S56. Recovery of *G'* (average of 10 consecutive thixotropic recovery cycles, Figure 5) of a fast-cooled 2.0 wt % 12-hydroxy-N-propyloctadecanamide in isostearyl alcohol gel in isostearyl alcohol gel at 25 ºC recorded in the linear viscoelastic regime (LVR, γ = 0.05 %, ω = 100 rad/s) after applying a destructive strain (γ = 30 %, ω = 1 rad/s; rotational strain was kept at 0 % for 0.05 s) and best single exponential rise fit (red line) according to eq 3 in the main text. (τ = 75 ± 16 s (R^2 = 0.96)).

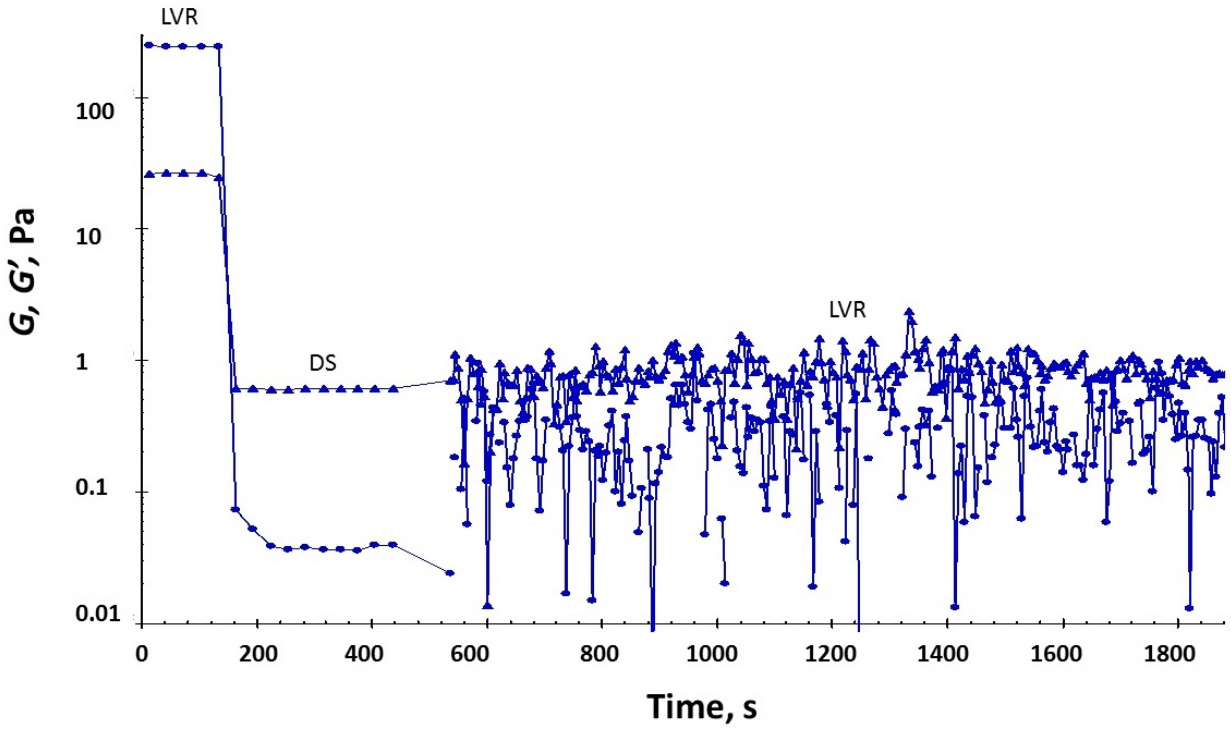

Figure S57. *G'* (▲) and *G"* (■) at 25 ºC as a function of time and application of different strains and frequencies to a fast-cooled 2.0 wt % **S-3-OH** in isostearyl alcohol gel. Linear viscoelastic region (LVR): strain = 0.05 %, ω = 100 rad/s. Destructive strain (DS): strain = 30 %, ω = 1 rad/s. Rotational strain was kept at 0 % for 0.05 s before changing from DS to LVR conditions.

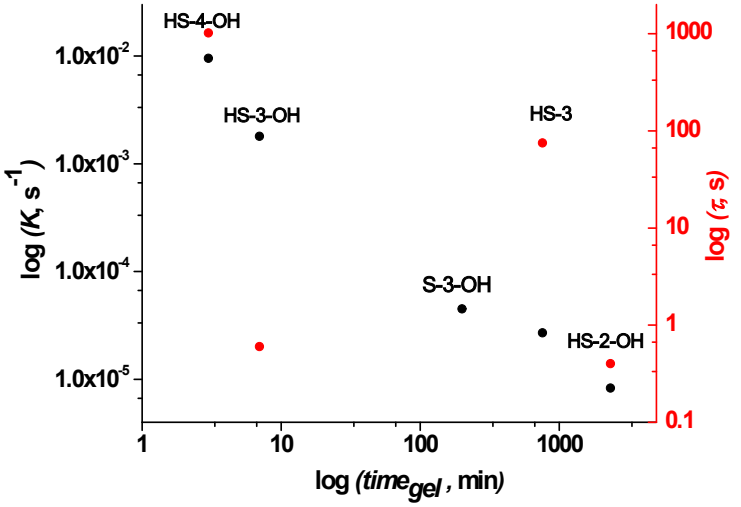

Figure S58. Log-log plot of $time_{gel}$ versus K (●) and τ (●) for 2 wt % isostearyl alcohol gels of **HS-n-OH** (**n** = 2, 3, 4), **S-3-OH** and **HS-3**. See Table 2 in the main text for details.

References:

[1] L. E. Alexander, *X-ray Diffraction Method in Polymer Science*, John Wiley & Sons, New York, 1969, pp 102-104.

[2] http://www.ncnr.nist.gov/

[3] S. R. Kline, *J. Appl. Cryst.,* 2006, **39**, 895-900.

[4] K. Serck-Hanssen, *Chem. Ind. (London),* 1958, 1554.

[5] V. A. Mallia, M. George, D. L. Blair and R. G. Weiss, *Langmuir,* 2009, **25**, 8615-8625.

[6] R. N. Butler, C. B. O'Regan and P. Moynihan, *J. Chem. Soc. Perkin I*, 1978, 372-377. .

[7] Drawn by adding the required atoms and bonds to single-crystal XRD structures of **HSA** methyl ester or *N*-(2-hydroxyethyl)octadecanamide using Mercury CSD 3.3 software.[a] Then, the geometry was optimized using PM7 in MOPAC2012.[b] a) C. F. Macrae, P. R. Edgington, P. McCabe, E. Pidcock, G. P. Shields, R. Taylor, M. Towler and J. V. D. Streek, *J. Appl. Cryst*. 2006, **39**, 453-457. b) J. J. P. Stewart, *J. Comp. Chem.,* 1989, **10**, 209-220.

[8] B. Dahlen, I. Pascher and S. Sundell, *Acta Chem. Scand. A,* 1977, **31**, 313-320.

[9] Using Chem 3 D Ultra 8 software (Cambridge Soft Corporation, USA) and adding the van der Waals radii of the terminal atoms according to: (a) A. J. Bondi, *Phys. Chem*., 1964, **68**, 441-451. (b) M. Mantina, A. C. Chamberlin, R. Valero, C. J. Cramer and D. G. Truhlar, *J. Phys. Chem. A*, 2009, **113**, 5806-5812.